AALBORG UNIVERSITY

DENMARK

Prostate Cancer Diagnosis using Magnetic Resonance Imaging - a Machine Learning Approach

Jensen, Carina

Publication date:
2018

Document Version
Publisher's PDF, also known as Version of record

Link to publication from Aalborg University

PROSTATE CANCER DIAGNOSIS USING MAGNETIC RESONANCE IMAGING – A MACHINE LEARNING APPROACH

BY
CARINA JENSEN

DISSERTATION SUBMITTED 2018

AALBORG UNIVERSITY
DENMARK

PROSTATE CANCER DIAGNOSIS USING MAGNETIC RESONANCE IMAGING – A MACHINE LEARNING APPROACH

Ph.D. Dissertation

by

Carina Jensen

AALBORG UNIVERSITY
DENMARK

Dissertation submitted October 2018

to the

Doctoral School in Medicine, Biomedical Science and Technology

at Aalborg University

SUMMARY

Prostate cancer (PCa) is the second most common cancer in men with one in every seven men developing the disease. The current diagnostic tools: PSA blood test, digital rectal examination (DRE), and transrectal ultrasound guided biopsies suffer from limitations of various degrees; elevated PSA level may indicate the presence of PCa, however, elevated PSA can also be caused by benign conditions. The DRE can only detect palpable lesions of certain size in the posterior aspect of the gland, but small lesions and those located in other parts of the prostate are missed. Due to the random nature of the biopsies, there is a risk of missing significant cancers, detecting insignificant cancers, and underestimate the aggressiveness of significant cancers.

Multiparametric magnetic resonance imaging (mpMRI) is being increasingly used to improve the diagnosis of PCa by reducing detection of clinically insignificant cancers and finding more clinically significant cancers that require treatment. mpMRI has shown useful for different applications within PCa diagnosis, including detection, characterisation, staging, treatment planning, and detection of recurrence.

The clinical analysis of mpMRI is however time-consuming, subjective, and requires high level of expertise that is not widely available. To overcome these limitations, research in development of automatic algorithms is conducted worldwide to aid the clinicians in their daily work. Automatic methods can simplify the reading task and reduce the reading time and variability.

The aim of this PhD thesis was to investigate automatic algorithms for PCa diagnosis using mpMRI. The thesis comprises three studies. The first study focuses on automatic detection of PCa using imaging features extracted from MRI. In the second study, PCa lesions are classified into level of aggression based on MRI imaging features to help the clinician in the risk stratification of the patient. The third study investigates an automatic algorithm for zonal segmentation of the prostate gland from the anatomical T2W imaging sequence.

This PhD thesis presents state-of-the-art arguing for the motivation and research objectives for the studies.

DANSK RESUMÉ

Prostatakræft er den anden mest almindelige kræftform ved mænd, hvor en ud af syv mænd udvikler sygdommen. De nuværende diagnostiske metoder: PSA blodprøve, digital rektal-undersøgelse (DRE) og ultralydsvejledte biopsier har begrænsninger af forskellige grader: et forhøjet niveau af PSA i blodet kan indikere prostatakræft, men det forhøjede niveau kan også være forårsaget af benigne tilstande. Da DRE kun kan detektere palpable cancere af en vis størrelse i den bageste del af kirtlen, vil små cancere og dem beliggende i andre dele af kirtlen blive overset. Tilfældigheden, hvormed biopsierne udtages, giver risiko for at overse klinisk betydelige cancere, detektere ubetydelige cancere og underestimere aggressiviteten af de betydelige cancere.

Multiparametrisk magnetisk resonance (mpMRI) billeder bliver i stigende grad anvendt til at forbedre diagnosen af prostatakræft ved at undgå at finde klinisk ubetydelige cancere og finde flere af de klinisk betydelige cancere, der kræver behandling. Inden for prostatakræftdiagnostik har mpMRI vist sig anvendelig til detektion, karakterisering, stageinddeling, planlægning af behandling og til at detektere tilbagefald af sygdommen.

Analysen af mpMRI er imidlertid både tidskrævende, subjektiv og kræver høj grad af eksperterfaring, som ikke er udbredt. For at løse disse udfordringer bliver der i stigende grad udviklet automatiske algoritmer, som kan hjælpe klinikeren i sit daglige arbejde. Automatiske algoritmer kan simplificere opgaven, reducere den tid, det kræver at analysere skanningerne, og begrænse variabiliteten mellem forskellige klinikere.

Formålet med denne ph.d.-afhandling var at undersøge automatiske algoritmer til brug ved diagnostik af prostatakræft ud fra mpMRI. Afhandlingen består af tre studier. Det første studie fokuserer på automatisk detektion af prostatakræft ud fra billedinformation fra MR-skanningerne. I andet studie bliver prostata cancere graderet automatisk ved hjælp af MRI billedinformation for en mere præcis risikovurdering af patienten. Det tredje studie undersøger en algoritme til automatisk zoneindtegning af prostata ud fra den anatomiske T2W MR-skanning.

Denne ph.d. præsenterer state-of-the-art argumenter for motivationen og forskningsformålene bag de tre studier.

TABLE OF CONTENTS

LIST OF ABBRIVATIONS

ADC   Apparent diffusion coefficient
AFS   Anterior fibromuscular stroma
AS   Active surveillance
AUC   Area under the receiver operating characteristic curve
BPH   Benign prostatic hyperplasia
bpMRI   Biparametric MRI
CAD   Computer-aided-diagnosis
CG   Central gland
CNN   Convolutional neural network
CT   Computed tomography
CZ   Central zone
DCE   Dynamic contrast enhanced
DRE   Digital rectal examination
DSC   Dice score coefficient
DWI   Diffusion weighted imaging
ECE   Extra capsular extension
ERC   Endorectal coil
GE   General electric
GG   Gleason Grade Group
GS   Gleason score
GT   Ground truth
KNN   K-nearest neighbour
LOOCV   Leave-one-out cress validation
mpMRI   Multiparametric MRI
MRI   Magnetic resonance imaging
MRS   Magnetic resonance spectroscopy
PCa   Prostate cancer
PI-RADS   Prostate imaging reporting and data system
PSA   Prostate specific antigen
PZ   Peripheral zone
QDA   Quadratic discriminant analysis
ROI   Region of interest
RP   Radical prostatectomy
RT   Radiation therapy
SNR   Signal-to-noise ratio
SVI   Seminal vesicle invasion
SVM   Support vector machine
T2W   T2-weighted
TRUS   Transrectal ultrasound of the prostate
TRUS+B   Transrectal ultrasound guided biopsies
TZ   Transition zone

PREFACE

This PhD dissertation is submitted to the Doctoral School in Medicine, Biomedical Science and Technology at Aalborg University as partial fulfilment of the requirements for the PhD degree.

The thesis represents the work conducted from July 2015 to October 2018 at Aalborg University Hospital, Department of Oncology, Department of Medical Physics. The work was supervised by Jesper Carl (main supervisor, July 2015-May 2016), Lasse Riis Østergaard (co-supervisor July 2015-May 2016, main supervisor May 2016-July 2018) and Niels Christian Langkilde (co-supervisor May 2016-July 2018).

Data used for the first part of this PhD work was obtained from Copenhagen University Hospital Herlev, generously provided by Lars Boesen, Herlev University Hospital. For the second part of the work, a public dataset from The Cancer Imaging Archive (TCIA) sponsored by the SPIE, NCI/NIH, AAPM, and Radboud University was used [1]. Third part used a public dataset by Lemaitre et al. [2].

The thesis consists of the following three papers:

A. C. Jensen, A.S. Korsager, L. Boesen, L.R. Østergaard and J. Carl. "Computer Aided Detection of Prostate Cancer on Biparametric MRI Using a Quadratic Discriminant Model." Scandinavian Conference on Image Analysis. Springer, Cham, 2017

B. C. Jensen, J. Carl, L. Boesen, N.C. Langkilde and L.R. Østergaard. "Assessment of Prostate Cancer Prognostic Gleason Grade Group using Zonal Specific Features Extracted from Biparametric MRI - a Machine Learning Approach", submitted to Journal of Applied Clinical Medical Physics, May 2018

C. C. Jensen, K.S. Sørensen, C.K. Jørgensen, C.W. Nielsen, P.C. Høy, N.C. Langkilde and L.R. Østergaard. "Prostate Zonal Segmentation in 1.5T and 3T MRI using a Convolutional Neural Network" submitted to Journal of Medical Imaging, August 2018

ACKNOWLEDGEMENTS

Pursuing a PhD degree has been a frustrating, rewarding and enjoyable experience. I would like to thank all the people who made it possible and an unforgettable experience for me.

First, I would like to thank my three supervisors throughout the course of my PhD study; Thank you, Lasse Riis Østergaard, for encouraging me through my research and for allowing me to grow as a researcher. I would also like to thank Niels Christian Langkilde for stepping in as co-supervisor in the middle of the process and helping me understand the clinical perspective of the research area. My gratitude to my former main supervisor, Jesper Carl, who gave me the opportunity to do this PhD and for helping and supporting me in the work.

I would also like to thank my co-authors of the papers that form part of this thesis for their help and contribution. Especially, Lars Boesen from Herlev Hospital who provided the data for the first study and gave constructive criticism, particularly within the clinical domain for the study plan and articles.

Thank you to all my colleagues at Department of Oncology and Department of Medical Physics, Aalborg University Hospital, for their support and all the great fun we have had through my employment there. Also, thank you to the people at the Department of Urology, Aalborg University Hospital, for showing me the clinical workflow for the patients. Thank you to the people in the Medical Informatics group at Aalborg University for letting me have an office space there and including me in social and scientific activities. Also, the Medical Image Analysis group at Aalborg University deserves some thanks for their help with various imaging challenges throughout my time as a PhD student.

Last but not least, thanks to my family and friends, thank you for listening, offering me advice, supporting and encouraging me through the course of the PhD.

CHAPTER 1. INTRODUCTION

One in every seven men will develop prostate cancer (PCa) making it the second most common cancer in men [3]. While most PCa lesions are slow-growing and non-fatal, some grow and spread quickly and with fatal outcome if left untreated [4]. A major challenge in PCa diagnosis is identifying patients with intermediate and high-risk cancers who need treatment while avoiding treatment of patients with low-risk cancers [5]. The current diagnostic tools; prostate-specific antigen (PSA) blood level, digital rectal examination (DRE) and ultrasound guided biopsies (TRUS+B), suffer from different limitations that lead to over- and undertreatment of the patients [6,7]. Multiparametric magnetic resonance imaging (mpMRI) has evolved as a promising diagnostic tool with superior performance compared to the aforementioned diagnostic methods in terms of information about size, location, and extent of the disease [8,9].

mpMRI enhances the detection of clinically significant PCa lesions, while reducing the detection of insignificant ones, and improves the risk stratification [10]. Because the analysis of prostate mpMRI requires high level of expertise, is time-consuming and affected by observer variation, automatic methods have been a rapidly growing area of research [11].

Over the past 10 years, automatic methods within prostate mpMRI analysis have evolved to simplify the task of the radiologist, reduce reading time and reader variability [12]. Automatic analysis of prostate mpMRI has many applications including detection of cancerous lesions for guiding the biopsy procedure, assessment of lesion aggressiveness, treatment planning of radiotherapy or surgical margin estimation before surgery and as imaging biomarker for treatment response [11].

The aim of this PhD work was to investigate automatic methods for the analysis of prostate mpMRI to aid clinicians in their daily work.

CHAPTER 2. BACKGROUND

This chapter gives an overview of prostate cancer (PCa), the diagnosis and treatment. Afterwards, the use and challenges of magnetic resonance imaging for prostate cancer diagnosis are described. Lastly, automatic methods for assessment of the magnetic resonance images are presented.

2.1. PROSTATE CANCER

PCa is the most common non-cutaneous cancer among men and one of the most common causes of cancer-related deaths [13]. The strongest risk factors for PCa are age, genetics and ethnicity [14]. The mean age of diagnosis is around 66 years and PCa rarely affects men under the age of 40 [15]. Most PCa are confined to the prostate gland and local tissue, referred to as localised or locally advanced PCa [14].

2.1.1. PROSTATE ANATOMY

The prostate is a gland of walnut-size, part of the male reproductive system that produces most of the fluid that makes up the semen. It is located anterior to the rectum and inferior to the urinary bladder [16].

The prostate gland is divided into four anatomical zones as shown in Figure 1. The peripheral zone (PZ) covers 70% of the gland and extends from the base (most cranial aspect of the gland) to the apex (most caudal aspect of the gland) of the prostate. The central zone (CZ) represents 25% of the gland and the transition zone (TZ) makes up the remaining 5%. On the anterior surface of the gland, a non-glandular region, the anterior fibromuscular stroma (AFS), is located, which represents the fourth anatomical zone. The urethra runs through the prostate where it conducts semen and urine from the ejaculatory ducts and bladder, respectively. The seminal vesicles are glands found on each side of the prostate which make most of the fluid in semen [7,16]. The PZ is the most common site of origin for PCa, where around 70% arises. The remaining cancers are located in the TZ (10-20%) and CZ (5-10%) [7]. TZ and CZ are commonly grouped together as the central gland (CG) [17].
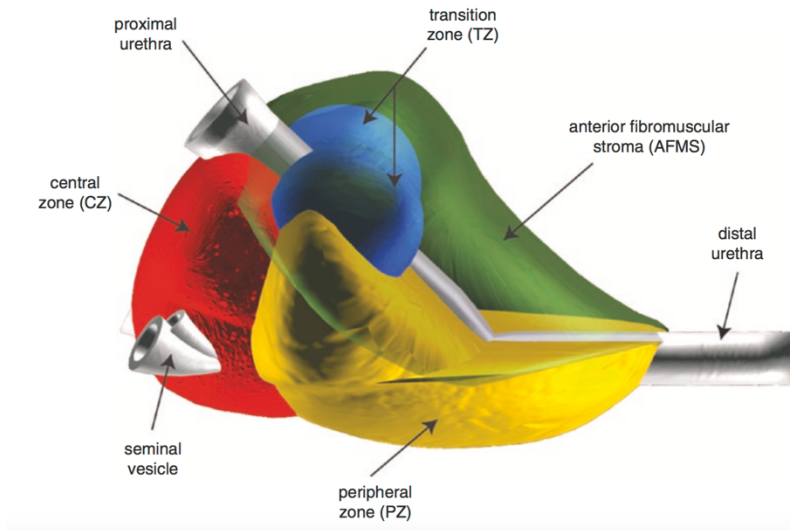
Figure 1. Anatomy of the prostate gland from a sagittal view. Retrieved from [7].

2.1.2. PROSTATE CANCER DIAGNOSIS

For patients with clinical suspicion of prostate cancer (PCa), with elevated prostate-specific antigen (PSA) and/or abnormal digital rectal examination (DRE), a set of transrectal ultrasound-guided biopsies (TRUS+B) are performed to confirm or reject the suspicion [18,19].

Prostate Specific Antigen

PSA is an antigen produced by normal, as well as malignant cells, of the prostate gland. An elevated PSA blood level is associated with PCa, however, benign conditions such as benign prostatic hypertrophy (BPH), prostatitis and other urinary symptoms can also cause an elevated level of PSA. The lack of specificity leads to over-diagnosis and overtreatment of PCa resulting in significant and unnecessary side effects. Studies have shown that approx. 20% of men with normal PSA levels have PCa, and many men with elevated levels do not [20,21]. PSA is, however, valuable in risk stratification of patients with confirmed PCa [22]. Calculation of e.g. PSA density (PSA divided by the transrectal ultrasound (TRUS) determined prostate volume) and PSA velocity (absolute annual increase in PSA) can be used as prognostic markers of the disease [21,23].

Digital Rectal Examination

Because the majority of PCa lesions are located in the PZ, DRE can be used to detect lesions of a certain size in that region. Lesions in other zones, however, cannot be reached by DRE [24]. As a suspicious DRE finding is predictor of more aggressive cancer it is a strong indicator for performing prostate biopsies and allows for identifying around 18% of men with PCa and PSA level below "normal". The DRE findings are, like PSA, also used for risk stratification [23].

Transrectal Ultrasound Guided Biopsies

The diagnosis of PCa is confirmed by needle biopsies of the prostate, see Figure 2. Gold standard is histological examination of 10-12 transrectal ultrasound guided biopsies (TRUS+B). The biopsies are obtained systematically, but randomly, from standard zones in the prostate [23]. Because most PCa lesions are not visible on TRUS, there is a high risk of missing clinically significant lesions, or the most aggressive part of it, leading to under-diagnosis, and thus possible under-treatment [25]. To overcome this high false-negative rate, patients often undergo one or more repeated biopsy procedure(s). This increases the cost of the procedure, risk of side effects and possibly increases anxiety and morbidity for the patient [26]. PCa detection rates for second, third, and fourth sets of biopsies are found to be 16.7%, 16.9% and 12.5%, respectively [27]. Conversely, there is a risk of over-detection, by coincidently hitting a clinically insignificant lesion during the random sampling. Thus, TRUS+B lack both sensitivity and specificity for the detection and staging of PCa patients [18,28].
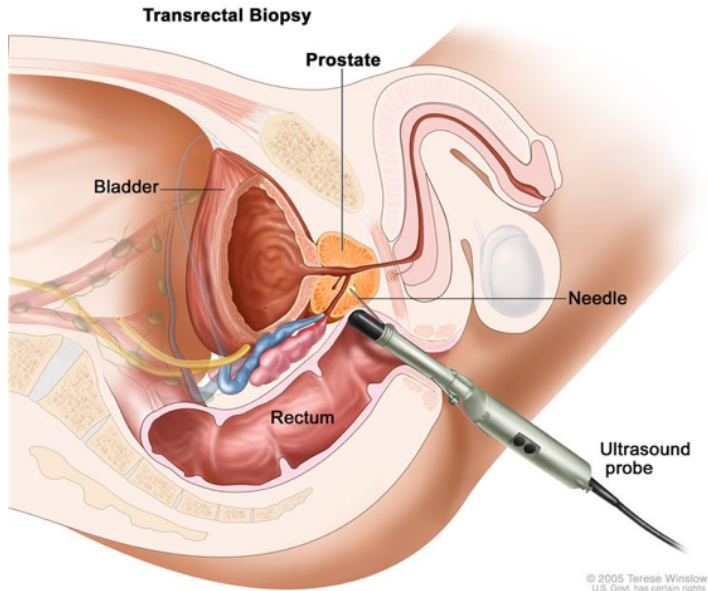
Figure 2. Transrectal ultrasound guided biopsy of the prostate. Retrieved from [29]*.*

Grading of Prostate Cancer

The histopathological aggressiveness of PCa is graded by the Gleason Score (GS), which is a powerful predictor of progression, mortality, and outcome of the disease. The Gleason system describes the architectural pattern of the tumour and the degree of differentiation of cells in the tumour. The architectural patterns of a lesion are graded on a scale from one to five and the sum of the primary (e.g. Gleason pattern 3) and secondary pattern (e.g. Gleason pattern 4) gives the total GS, e.g. GS 3+4 = 7. A simplified drawing of the five different Gleason patterns can be seen in Figure 3 with pattern one showing small, uniform glands and gradually being more irregular and less differentiated for increasing pattern scores. Higher GS indicates higher level of aggression with worse prognosis [30]. The GS from prostate biopsies is used for clinical decision making, treatment selection, and prediction of outcome for patients. However, due to the random nature of TRUS+B, the GS from the biopsies often differ from that determined after surgical removal of the prostate (Radical prostatectomy (RP)) [31].
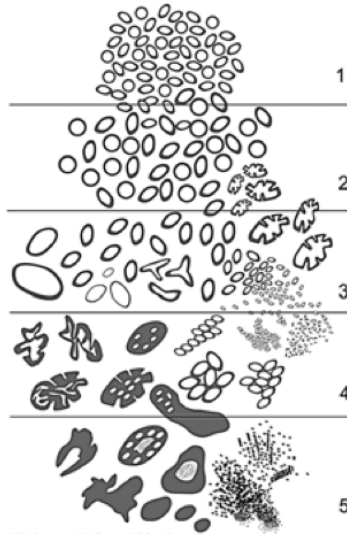
Figure 3. The five prostate histological Gleason patterns. Modified from [32]

The Gleason grading system was developed by Donald Gleason and has evolved significantly from its original in 1960s-1970s [33,34]. Table 1 shows the Gleason score and patterns together with the recently internationally accepted concept of Grade Groups [23,32].

Table 1. The relationship between the recently accepted Grade Group system, Gleason score system and Gleason patterns.

Grade Group	Gleason Score	Gleason Pattern
1	≤6	≤3+3
2	7	3+4
3	7	4+3
4	8	4+4, 3+5, 5+3
5	9 or 10	4+5, 5+4, 5+5

The concept of Grade Groups offers greater prognostic value and more accurate reflection of the PCa biology compared to the previous system [16]. A GS 7 is

considered intermediate risk for many clinicians; however, studies show that GS 3+4 = 7 demonstrates better outcome than GS 4+3 = 7. Furthermore, the previous Gleason systems can be misleading for the patients e.g. a GS 6 could be falsely assumed to be in the mid-range of aggressiveness, even though it is the lowest Gleason score used for defining aggressiveness (Grade Group 1) [30,35].

2.1.3. PROSTATE CANCER TREATMENT

Based on the clinical parameters, such as PSA, DRE, GS/Grade group from TRUS+B and the overall health, age, family history and ethnicity of the patient the clinician recommends a plan of treatment [23]. Each treatment choice has benefits and risks which must be considered and there is seldom just one right choice of treatment [36].

As PCa ranges from a nonsignificant indolent to an aggressive form of cancer with fatal outcome, the treatment options include both radical and conservative approaches. Patients with a low risk PCa may never need radical treatment and is instead offered a conservative treatment approach, such as active surveillance (AS), which includes regular follow-up PSA tests, DRE and TRUS+B to monitor potential progression. If the disease progresses the patient can be referred to radical treatment. The purpose of AS is to achieve the correct onset of curative treatment, however, radical treatment can also be triggered upon the request of the patient [23].

Radical treatment of PCa should be based on probability of progression, side effects and potential benefit to survival [23]. Two main radical treatment options exist; external beam radiation therapy (RT) (often in combination with hormone therapy) and radical prostatectomy (RP) [37,38].

RT uses high energy X-ray beams to destroy the cancerous cells while sparing as much of the normal surrounding tissue as possible [39]. RP is surgical removal of the prostate gland, including seminal vesicles and nearby lymph nodes [7]. RT and RP have significant side effects, such as impotence, incontinence and damage to the bladder and rectum [40].

Many patients diagnosed with PCa undergo radical treatment even though their disease unlikely will cause decrease in life expectancy leading to unnecessary side effects from the treatment [41]. On the other hand, patients that undergo conservative treatment, like active surveillance, endure the psychological burden of living with untreated cancer and 20-50% initially selected for AS convert to radical treatment due to incorrect initial risk stratification [42,43]. Thus, better risk stratification is a key challenge in PCa research [44].

2.2. MULTIPARAMETRIC MAGNETIC RESONANCE IMAGING OF THE PROSTATE

Multiparametric magnetic resonance imaging (mpMRI) is a combination of morphologic and functional MRI sequences. The diagnostic value of mpMRI for PCa diagnosis is well established by recent scientific work and ranges from initial detection of clinically significant cancers, to evaluation of biological aggressiveness, accurate staging and detection of recurrence [7,45].

In patients with previous negative TRUS+B and continued suspicion of PCa, mpMRI has shown particular useful for guiding biopsies towards cancer suspicious areas, why it is now included in clinical guidelines e.g. European Association of Urology (EAU) guideline on PCa [46]. mpMRI guided biopsies increases the detection of clinically significant cancers by 12%, can significantly reduce the number of performed biopsies (up to 28%) and decrease the detection of low-risk PCa in men with elevated PSA compared to standard TRUS+B [10,47,48]. Thus, reducing overdiagnosis and thereby avoid side effects associated with treatment.

A correct assessment of the PCa stage is crucial for correct management of the disease [49]. Between 24% and 46% of patients staged with clinical nomograms are routinely under staged [50]. mpMRI has been found to improve the detection of extra capsular extension (ECE) and seminal vesicle invasion (SVI) compared to these nomograms [49,51,52]. Presence of ECE affects the long-time prognosis negatively and is therefore essential pre-therapeutic information. Patients with SVI are often not candidates for RP and for patients referred for RT the radiation field should include the seminal vesicles. The sensitivity of mpMRI for ECE detection is poor, especially for less experienced readers, since it cannot detect microscopic ECE [23]. The specificity on the other hand is high, why it can be used in the treatment planning of patients without signs of ECE [7,49].

The GS from TRUS+B is used for treatment planning and risk assessment of the patient. This GS can, however, be incorrect due to biopsy sampling error, why mpMRI has been investigated to improve the pre-therapeutic assessment of GS. For identifying GS ≥7 mpMRI is particular accurate [23,53,54]. Several studies have shown correlation between mpMRI parameters, such as the apparent diffusion coefficient (ADC), and the GS. Due to considerable overlap in the values, it cannot yet be used alone for clinical decision making but can be used as an additional parameter in management of PCa patients [55–57].

Studies have investigated the use of mpMRI for determining the PCa volume as it is a well-known prognostic factor and mandatory for successful focal therapy that aims to treat only the index lesion while sparing the remaining gland and surrounding tissues [58,59]. The studies have shown that mpMRI can give a fairly accurate estimation of the PCa volume, however, larger PCa (>10mm and >0.5cc in volume) show more accurate estimation than small ones [60,61].

Transrectal ultrasound (TRUS) has been found to underestimate the prostate volume, and since the volume is used to calculate PSA density, this results in an inaccurate calculation. MRI gives a more accurate estimation of prostate volume compared to TRUS and can therefore give a better estimation of PSA density [62].

For RT and RP planning, multiple studies have shown potential of mpMRI. mpMRI can help define surgical margins, select patients eligible for nerve-sparing operation, and create more accurate delineation of target volume for RT [23]. Focal therapies are emerging as it offers less morbidity with attaining disease control. mpMRI enables the clinician to identify the exact extent and location of the PCa, and the focal therapy can thereby be delivered with precision [63,64].

Also, mpMRI is increasingly being used for selecting patient eligible for AS as it provides high risk-assurance to the clinician [43,65]. Furthermore, mpMRI may also help identify disease progression in patients enrolled in AS, however, a key challenge is to define radiological progression that should prompt a change from AS to active treatment [65].

For patients who develop biochemical recurrence salvage treatment can be an option. Early detection of recurrence is crucial for patient survival [66]. mpMRI has shown promising results for detection of disease residual or recurrence following RT, RP and focal therapy [7,66]. Especially the diffusion-weighted imaging (DWI) and dynamic contrast-enhanced (DCE) sequences are useful for detection of recurrence. The DWI sequence shows evident restriction and the DCE sequence shows presence of contrast uptake [67].

Currently, the use of mpMRI as a triage test is increasingly being investigated. Patients with negative mpMRI are likely to have no clinically significant PCa and could potentially avoid biopsy. If mpMRI is used as a triage test, 27% of patients could avoid biopsy, and fewer (5%) clinically insignificant PCa would be diagnosed [68–70]. However, young patients with high or increasing PSA should still undergo standard TRUS+B until a definitive conclusion about the negative predictive value of mpMRI has been drawn [71].

2.2.1. MRI ACQUISITION

Typically, an mpMRI examination consists of an anatomical sequence (T2-weighted (T2W)) and different functional sequences, usually DWI and DCE sequences. The choice of sequences is based on the clinical indication and cost and time constraints [72].
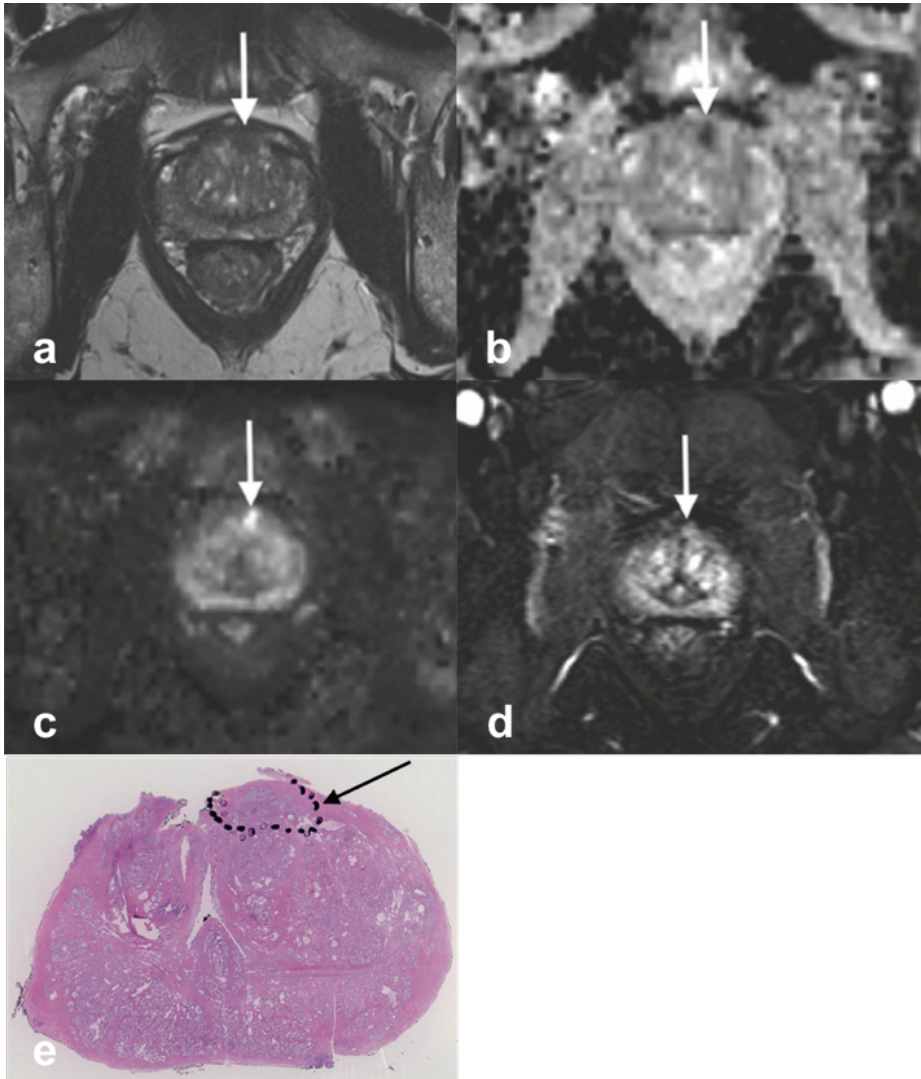
Figure 4. Multiparametric MRI of the prostate gland with a cancer lesion (white arrow) in the anterior fibromuscular stroma. a) axial T2W, b) ADC, c) DWI, d) DCE and e) surgical specimen showing a Gleason score 4+3 (black arrow). Modified from [7]*.*

Usually, prostate mpMRI is performed in high-field magnets (1.5T or above). Using a 3T magnet benefits from higher signal to noise ratio (SNR) compared to 1.5T scanners. Endorectal coil (ERC) is recommended for 1.5T scanners to increase SNR,

however, it causes deformities of the prostate gland and is uncomfortable for the patient [7,73].

T2W

The T2W images provide high spatial resolution and permit the evaluation of prostate zonal anatomy and can clearly differentiate the PZ from the CZ and TZ in young male subjects. In aging men benign prostatic hyperplasia can cause the signal intensity to vary, making the zones more difficult to discern [9]. PCa appear as "erased charcoal" on T2W imaging (see Figure 4a), however, benign abnormalities such as post-biopsy haemorrhage, fibrosis and prostatitis can mimic the appearance of PCa, especially in the PZ [7]. T2W imaging is the dominant sequence for detecting PCa in the TZ according to the newest version of the PI-RADS guidelines (Prostate Imaging Reporting and Data System v2) which is a structured reporting scheme for the evaluation of PCa on mpMRI [74]. Some studies have shown correlation between the intensity decrease in T2W and the Gleason score of the lesion, thus showing potential for risk stratification [75]. Also, T2W images are used for local staging of PCa, as they allow detection of extracapsular extension (ECE), invasion of seminal vesicle and nodal involvement [7].

DWI

DWI is the dominant imaging sequence for PCa appearing in the PZ based on the PI-RADS v2 guidelines [74]. DWI measures random Brownian movement of water molecules in the tissue thereby indirectly reflecting tissue cellularity. PCa tissue has increased cellularity compared to normal tissue leading to a high signal intensity (hyperintense) on DWI (see Figure 4c). DWI is usually performed with at least two different b-values (lowest b-value at 50-100 sec/mm^2 and highest $\geq$ 1400sec/mm^2), where b is the strength of the diffusion gradient. The highest b-value is usually preferred for detection of PCa, since noise and signal decay increase with the b-value [7].

ADC

The DWI sequence enables calculation of the apparent diffusion coefficient (ADC), which measures the degree of water diffusion in the tissue. Two or more b-values are needed for ADC calculation. PCa shows low signal intensity (hypointense) on ADC (see Figure 4b) and the lower the ADC value, the higher the likelihood of a more aggressive lesion [76].

DCE

The DCE sequence is performed after administration of a gadolinium contrast agent to evaluate differences in enhancement between normal and cancer tissue [77]. Contrast is taken up and released more quickly in PCa cells due to angiogenesis, which is the formation of new capillaries from the existing blood vessels [78]. For tumours to develop, grow, and progress into metastasis, the process of angiogenesis is important, hence DCE has been used as a marker hereof [7,79]. The DCE-MRI sequence has shown particularly useful for the detection of recurrences which show enhancement within the scar tissue [80].

Biparametric MRI

Although the latest version of the PI-RADS guidelines has ascribed the DCE sequence a minor role in determining the PI-RADS score, it is still recommended as part of the MRI examination [74,81]. The disadvantages of DCE imaging includes administration of expensive contrast agent, long scan time, the possibility of an allergic reaction to the contrast agent, lack of reproducibility of the quantitative parameters and the extra burden of radiologist to analyse the images. Due to the fast increase in the use of mpMRI for PCa, a biparametric MRI (bpMRI) protocol, including only T2W and DWI is actively being evaluated for PCa diagnosis. The bpMRI protocol can be performed in approx. 15 minutes, avoids the intravenous injection of expensive contrast medium while maintaining adequate diagnostic accuracy, all of which could encourage a greater use [81–83].

2.3. CHALLENGES IN PROSTATE CANCER DIAGNOSIS USING MRI

Despite the increased diagnostic accuracy for PCa using mpMRI, different challenges have hindered widespread adoption of mpMRI for PCa diagnosis.

2.3.1. STANDARDISATION

The quality of PCa mpMRI is largely dependent on the scanner used (vendor, magnet field strength, protocol, software etc.), patient factors (movement, preparation strategy etc.), and, most importantly, the interpretation by the radiologist [45]. The Prostate

Imaging-Reporting and Data System version 2 (PI-RADS v2) aims to simplify and standardise the image acquisition and interpretation of PCa mpMRI [74].

2.3.2. PERSONNEL, INTER- AND INTRA-READER VARIABILITY

Even with a standardisation of the acquisition and interpretation, certain pitfalls in the interpretation exist; such as benign conditions, artefacts due to the ERC, or changes in appearance after treatment. High level experience in prostate mpMRI is crucial for accurate management, which is not available in many centres [7,67]. Furthermore, inter-reader variability is a challenge, even for expert readers [23,84].

2.3.3. COSTS

mpMRI is a rather expensive examination and upfront the costs are high. The ability of mpMRI to prevent biopsies, reduce overtreatment thus reduce unnecessary side effects and lead to higher quality of life, may result in overall cost-effectiveness, however, further studies are necessary to confirm this [10,85].

Reducing the mpMRI protocol to bpMRI could reduce scan time from 40 to 15 mins, avoid the use of contrast medium, and thereby lower the costs [81].

2.4. COMPUTERISED METHODS

The use of MRI for PCa diagnosis requires the radiologists to read enormous amounts of images and requires expertise knowledge which is not widely available. Automatic methods could simplify the task of the radiologist, reduce reading time and reader variability [12]. Automatic methods have been found to help less experienced mpMRI readers obtain same level of performance as experienced readers for PCa analysis [86].

Development of automatic methods for PCa analysis on mpMRI has been an active field of research with two reviews in 2015 presenting the current literature on computer-aided diagnosis (CAD) systems for PCa analysis including more than 270 references [2,87]. In 2016 another review on the subject was published including 200 references [11]. Common components in automatic systems for PCa diagnosis include preprocessing, image registration, segmentation, detection and classification. A typical workflow for automatic PCa analysis on mpMRI is shown in Figure 5.
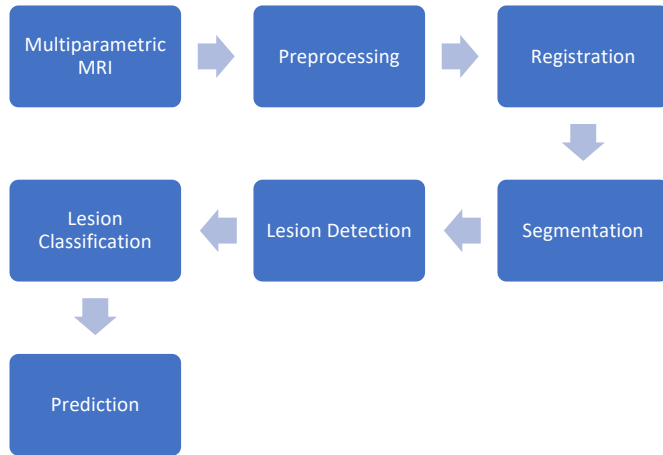
Figure 5. Flowchart showing a typical workflow for automatic systems for prostate cancer diagnosis using multiparametric MRI.

2.4.1. PREPROCESSING

Preprocessing of the images includes normalisation of image intensities, where especially the T2W image sequence suffers from inter and intra patient variation, even for images obtained using the same scanner and protocol. Other common preprocessing methods include noise filtering and bias field correction [11]. The choice of preprocessing steps depends on the dataset and application.

2.4.2. REGISTRATION

Registration, which is the process of aligning two or more images, can be useful to account for patient movement and changes in bladder/rectum filling during the examination. MRI examination protocols with a long time frame (e.g. DCE imaging) increase the likelihood of significant patient movement and thus image registration [87].

2.4.3. SEGMENTATION

Segmentation of the prostate from MRI plays an important role in PCa diagnosis [88–92]. The lack of clear boundary and significant variation in prostate shapes and appearances make manual delineation a challenging task. It is well established that the T2W imaging sequence offers the best assessment of prostate anatomy and ability to delineate the margins and differentiate between the zones of the prostate gland [93]. The manual delineation is highly time-consuming and requires experience in prostate MRI. Automatic methods in the literature includes atlas based, model based (e.g. active shape model), edge based and combinations hereof [94].

In recent years, approaches based on deep convolutional neural networks (CNN) have made significant progress in medical image analysis, including prostate segmentation [95–97]. Current first place in MICCAI grand prostate MRI segmentation challenge (PROSTATE12) is a CNN approach (achieving a Dice score coefficient of 0.8721) [89].

Lately, automatic zonal segmentation of the prostate has gained more focus. The majority of PCa is located within the PZ, and because the biological behaviour of the PCa differs between zones, this information is extremely important for clinical decision making [98–101]. Current studies on zonal segmentation have used different approaches such as voxel (3D analogue of a pixel) classification and active shape models [102–110]. One of the major challenges in zonal segmentation is the lack of features and gradients in the apex and base of the gland [97,111].

2.4.4. DETECTION

The initial work on automatic methods in prostate mpMRI , starting in 2003 by Chan et al., focused on highlighting suspicious areas for targeted MRI guided biopsies [112]. The most common approach in the literature is classification of voxels as either being PCa or normal tissue based on different imaging features such as texture, signal intensity and gradient information. The T2W sequence is the most commonly used for PCa detection algorithms since it is available for most patients [2]. A study by Rampun et al. investigated 215 texture features from T2W MRI for classifying voxels in the PZ as malignant and benign using 11 different classifiers (e.g. support vector machine (SVM), random forest, naïve Bayes and k-nearest neighbour) [113]. Combining the T2W sequence with one or more functional sequences offers improved detection over a single image modality. Image features extracted from T2W, DCE and DWI resulted in AUC of 0.95 in a study by Peng et al. using a linear discriminant analysis for classifying regions of interest as either cancer or normal [114]. Most studies use T2W MRI in combination with DWI, including ADC, and/or DCE imaging, however, magnetic resonance spectroscopy imaging (MRS) has also been investigated. The MRS has not gained wide acceptance probably due to the complexity and length of data acquisition [11]. Several studies agree that a zone-aware

classifier significantly improves the detection of PCa [115,116]. The majority of published PCa detection algorithms report an area under the receiver operating characteristic curve (AUC) between 0.80 and 0.89 [87]. The study by Peng et al. presented above is among the studies representing the highest performance in the literature.

2.4.5. CLASSIFICATION

For PCa patients the choice of treatment is based on clinical factors, such as PSA level, GS, age and comorbidities. As mentioned earlier, the GS is the most powerful predictor of progression, mortality, and outcomes of the disease. Because the GS from prostate biopsies often differ from the true GS from RP, there is a clinical need to better differentiate slow-growing, indolent PCa from those of clinical significance with fatal outcome [11]. mpMRI can potentially be used for non-invasive, pre-treatment assessment of PCa aggressiveness. There is a significant correlation between GS and ADC values, with lower ADC values indicating higher GS. Other studies have also found correlation between DCE parameters, T2W signal intensity and PCa aggressiveness. These single parameters, however, are not sufficient alone to predict the GS [117–122]. Several studies have investigated algorithms with multiple imaging features, such as texture, intensity from T2W, DWI and ADC to differentiate malignant from benign lesions, or classify lesions into clinically insignificant (GS≤6) or clinically significant (GS≥7) with promising results [123–129]. A study by Holtz et al. investigated a three-class classifier (low, intermediate and high grade) and compared it to a two-class system and reported low performance for the three-class system. One study achieved accuracies up to 0.93 for two-class classification of GS≤6 versus GS≥7, and 7 (3+4) versus 7 (4+3) by using features extracted from ADC and T2W imaging [126]. Sensitivity of 100% and specificity of 76.92% was achieved in a more recent study based on multimodal convolutional neural network for separating GS≤6 from GS≥7 [127]. Because the prognosis and therapeutic options differ for each GS grading, more accurate differentiation of lesions into more than 2 or 3 classes would be of clinical interest.

CHAPTER 3. BACKGROUND SUMMARY AND THESIS OBJECTIVES

Prostate cancer (PCa) is the most commonly diagnosed cancer among men except for skin cancer. Because the current gold standard in PC diagnosis has high risk of both under- and over-diagnosing the patients, mpMRI is increasingly used to improve the diagnosis. The number of prostate MRIs in Europe is increasing very fast which sets high demands to the radiologists. Furthermore, the interpretation of mpMRI requires a high level of expertise that is not readily available, is time consuming and affected by significant interobserver variation. Thus, there is a demand for accurate automatic methods that decrease reading time, reduce required expertise in radiology reading, and offer a consistent risk assessment in prostate mpMRI.

Therefore, the motivation for this PhD study was to investigate the use of machine learning based methods for diagnosing prostate cancer in mpMRI that can bring objectivity and potentially ease the daily work flow for physicians.

The objectives of this thesis are:

- Automatic detection of prostate cancer lesion in MRI (disseminated in **Paper A)**

- Classification of prostate cancer lesion into Gleason grade group based on imaging features extracted from MRI (disseminated in **Paper B**)

- Automatic zonal segmentation of the prostate gland from T2W MRI (disseminated in **Paper C**)

CHAPTER 4. RESEARCH METHODOLOGY - MACHINE LEARNING

This chapter gives an introduction to general machine learning concepts within medical imaging together with an overview of the methods used for the three studies in the PhD work.

Machine learning algorithms are computer algorithms that have the ability to learn a specific pattern from the data (in this case, prostate mpMRI) in order to do classification. Machine learning approaches are increasingly being used in medical image analysis for clinical applications [130,131]. Within medical imaging, the input data are multiple radiomic features (i.e. information in the image, interesting for the task at hand) which are related to an outcome (e.g. cancer versus normal tissue) [132]. The processes in many machine learning algorithms include feature extraction and selection, classification, and model validation, as shown in Figure 6.
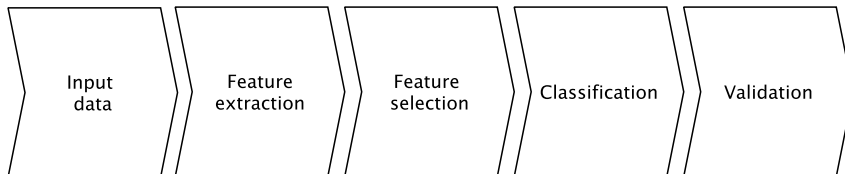
Figure 6. A typical machine learning process.

4.1. FEATURE EXTRACTION

The process of finding discriminative information for classification is called feature extraction. Image features can be extracted voxel-wise or region-wise, where the region can be the full image or a region of interest (ROI) within the image (e.g. a cancer lesion). For PCa analysis on mpMRI the majority of studies have extracted intensity as a feature often in combination with histogram, edge- or texture-based features [2]. For the first study (**Paper A**) a combination of intensity and gradient (edge-based) features was extracted from T2W, ADC and DWI image sequences. The signal intensity in all three image sequences is interesting as PCa often shows lower signal intensity in T2W and ADC, and higher signal on DWI, compared to non-

cancerous tissues. Several studies have found edge-based features, like Prewitt, Sobel, Kirsch and Gabor, to be discriminative of PCa [2]. Sobel gradient features were included in study one (**Paper A**) as PCa often shows as focal low (T2W and ADC) or high intensity (DWI) lesions [7]. Furthermore, the distance from each voxel within the prostate to the prostate boundary was used as feature, since the probability and appearance of PCa is based on the location in the gland [11].

For the second study (**Paper B**) a combination of histogram and texture features was used for the classification of PCa lesions into grades of aggressiveness. Texture features have been extensively studied in medical image analysis, despite the pathophysiology behind not being fully understood [117]. Fourteen Haralick texture features and eleven grey level run length texture features derived by Galloway were extracted from each ROI in the T2W and DWI image [133,134].

Several histogram features from mpMRI have shown to correlate with the Gleason score; the features alone, however, cannot be used for accurate prediction of the Gleason score [128]. Because the appearance of PCa differ between the zones, the extracted features differed based on the zonal location of the lesion for study two (**Paper B**).

4.2. FEATURE SELECTION

Feature selection is the process of selecting the most discriminative features and remove redundant or noisy features that add no relevant information for a specific classification task. Feature selection is important, especially for high dimensional datasets, to avoid overfitting (see section 4.7) and improve model performance. A review of feature selection methods has been published by Saeys et al. presenting advantages and disadvantages of the different methods [135]. Methods of feature selection includes filter, wrapper and embedded methods [135].

Filter methods apply a statistical measure to each feature, such as correlation or p-value, to rank the feature to be kept or removed. The advantages of filter methods are the simple and fast computations together with the classifier independence. Wrapper and embedded methods interact with the classifier and model the dependencies between features. These methods have a risk of overfitting and are dependent on the selected classifier. Examples of wrapper and embedded methods are sequential forward selection and decision trees [135].

An exhaustive search through the feature space will reveal the optimal feature set. This is, however, not computationally feasible for a large number of features, as the number of feature combinations is 2^n, n being the number of features in the whole set [136]. In addition to the disadvantages mentioned for the above-mentioned feature selection methods, they also have the risk of getting stuck in local optimum during the feature search, which prevents convergence toward a global optimal solution [135]. A

semi-exhaustive feature search was used in study two (**Paper B**) in order to find a semi-optimal feature set for the classification task. One to six features were used in each combination to reduce risk of overfitting and to limit the computational requirement. The approach resulted in 584,934 feature combinations to be evaluate in the model.

4.3. CLASSIFIERS

The aim of the classifier is to assign a class or label to a sample, e.g. an image voxel, based on the input data. Two main types of classifiers exist: supervised and unsupervised, based on how they analyse the data. Supervised classifiers are the most commonly applied to medical images, where a label is known for each training sample, as opposed to unsupervised classifiers that find hidden patterns without any labels for the training data [132]. Several classification algorithms are available, and the choice depends on the application and nature of the dataset. Different classifiers have been used for prostate MRI including sparse kernel methods (e.g. support vector machines), linear models (e.g. linear discriminant analysis), probabilistic (naïve Bayes) and ensemble learning (e.g. random forest) [2]. S.E. Viswanath compared 12 different classifiers for PCa detection on MRI and found a quadratic discriminant analysis (QDA) to give the best overall performance [137]. Therefore, the QDA classifier was used for the first study (**Paper A**). The k-nearest neighbour classification algorithm (KNN) is a simple classifier which uses the distance between the training samples and the new data point as similarity measure to assign a class [138]. For study two (**Paper B**) KNN was chosen due to speed and the fact that it works well on small datasets.

4.4. DEEP LEARNING

A special subcategory of machine learning is deep neural networks. These networks are inspired by the structure and function of the brain and the term "deep" refers to the number of hidden layers in the network. Neural networks have shown promise in a variety of applications within e.g. computer vision, speech recognition and medical image analysis. For imaging tasks convolutional neural networks (CNNs) are the most commonly applied type of networks as they capture the information among neighbouring pixels (spatial relationship) which is valuable information. The CNNs have the benefit of eliminating the need for user extracted features, as this is part of the search process of the network (see Figure 7) [139].
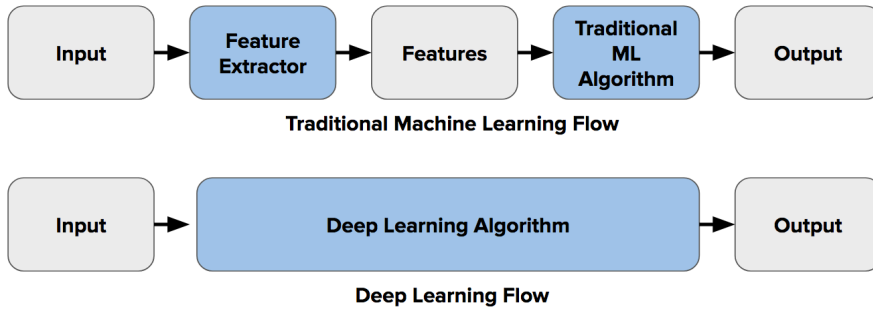
Figure 7. The difference in workflow between traditional machine learning and deep learning. Retrieved from [140]*.*

The common architecture of a CNN can be seen in Figure 8 and consists of an input and output layer with multiple hidden layers in between. The hidden layers are typically convolutional layers followed by pooling layers, and fully-connected layer(s) at the end. During the convolution and pooling operations, the network captures the image features (e.g. edges, colour and texture) of the input image. A filter (or kernel), often a 3x3 matrix, is sliding over the image for every position and calculating the dot product. This results in an activation map (or feature map) and is repeated for each filter and called the convolution operation. The number and size of the filters are user determined together with the network architecture. The fully-connected layer(s) at the end, which performs non-linear transformations of the extracted features, is used to assign probability of each class to make a prediction [131,139,141].
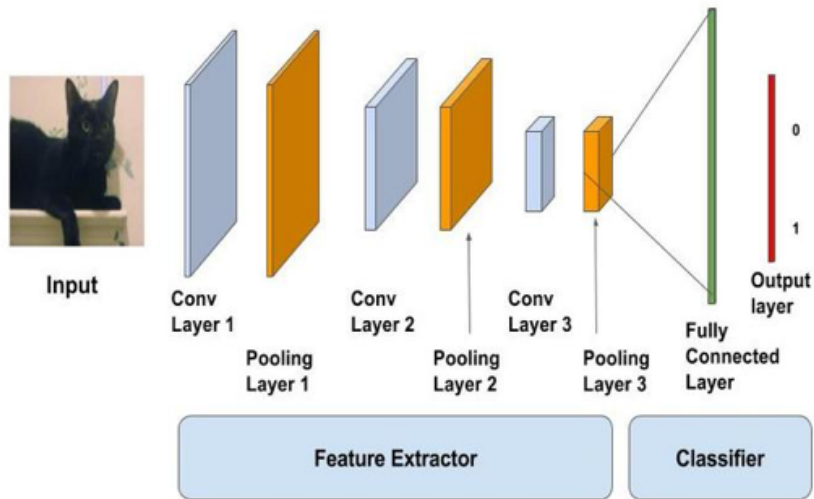
Figure 8. A typical convolutional neural network architecture. An image is fed to the convolutional neural network to assign a probability of the image being a cat. The Conv layers (convolution layers) together with the pooling layers extract the image specific features which are used for classification by the fully-connected layer. Retrieved from [142].

The advances in computational performance and substantial increase in available data has led to remarkable success in CNN [96]. Within medical imaging the number of available annotated training images is still limited compared to the sample size used for CNN for successful training. A CNN architecture, called the U-net Ronneberger et al, has shown promise within medical image segmentation of relatively small datasets and for different applications [143]. The U-net architecture was used for the third study (**Paper C**) for the zonal segmentation of the prostate with some modifications to the original architecture which are described in the article (**Paper C**). Different hyperparameters can be optimised for a CNN (e.g. learning rate, number of epochs and batch size), and improved model performance can be achieved by finding the optimal values. However, the tuning of the hyperparameters is considered less important than the choice of network architecture and the preprocessing techniques used for the images [96].

4.5. EVALUATION MEASURE

To evaluate the performance of a model, several metrics can be used. For classification of voxels or lesions, it is possible to compute the components in the confusion matrix. From this, the accuracy, sensitivity, and specificity can be

calculated. The sensitivity and specificity can be used to calculate the AUC which is often reported and used to compare models. The AUC is the area under the receiver operating characteristics curve which shows the sensitivity as a function of (1-specificity) for varying thresholds of the classifier [2,144]. AUC was used as evaluation metric in study one (**Paper A**) and study two (**Paper B**) for comparison with models in the literature. Other supportive metrics such as the accuracy, sensitivity, and specificity were also reported in study two (**Paper B**). In study one (**Paper A**), the number of falsely detected lesions and percentage false positive voxels were also reported.

In segmentation tasks the most common metric is the dice score coefficient (DSC) which is a measure of overlap ranging from 0, indicating no overlap, to 1, indicating a complete overlap. The DSC is calculated as two times the overlay between the segmentation and ground truth, divided by the sum of the number of elements in the segmentation and ground truth. In study three (**Paper C**), the DSC was used to evaluate the segmentation results. Other measures include the Jaccard coefficient and distance measures e.g. Hausdorff distance measuring the closeness of two sets of points [89].

4.6. MODEL VALIDATION

A simple approach for validating a model is to randomly divide the dataset into a training set and a validation set. This approach has the drawback of being highly dependent in on which samples (in this case, patients or lesions) are included in each set. Furthermore, only part of the data (the training set) is used to fit the model which can result in inferior performance compared to training on the full dataset. A common strategy for evaluation of model performance that addresses the latter issues is cross-validation [144]. Leave-one-out cross validation (LOOCV) is one type of cross-validation often used for small datasets. From the full dataset one patient is held out for validation while the remaining patients are used for training. This process is repeated until all patients have been used for validations. This validation technique was used for the first study (**Paper A**) due to the small sample size. For larger datasets LOOCV is computationally expensive. Another popular validation method is k-fold cross-validation where the dataset is split into k folds, and each fold is retained as the validation data for the model while the remaining data is used for training. This is repeated k times, and the performance of the model is reported as the average of all folds [2,144]. k-fold cross validation was used to validate the models in study two (**Paper B**) with k=3. In study three (**Paper C**) 5-fold cross-validation was used.

Optimally, an independent test set is available after model validation to evaluate the true performance of the model [145]. This is, however, often not possible due to the limited number of patients normally available in medical image analysis. The choice of validation procedure should be based on the problem at hand [146].

4.7. OVERFITTING

Overfitting is the phenomenon of a classifier fitting the training data too tightly and thereby losing the ability to generalise to new samples. The risk of overfitting increases with the number of features, especially for smaller datasets. Controlling overfitting is a challenging task in machine learning. Techniques to reduce the risk of overfitting include: larger sample size, smaller number of features, using a simpler model, and cross-validation techniques. The sample size can often not be affected in medical imaging tasks as large datasets are either unavailable or expensive to acquire. The number of features is decided during the feature selection process, and using a small number of features will reduce the risk of overfitting. Choosing a simple model, i.e. low number of learnable parameters for the classification task can also be considered, however, using too simple a model can result in poor performance. Methods such as k-fold cross validation and LOOCV described in section 4.6 are widely accepted for model evaluation to prevent overfitting. [144,147,148]

CHAPTER 5. PAPER CONTRIBUTIONS

This chapter presents a summary of the three studies conducted as part of this PhD thesis.

The thesis is based on three original studies all focusing on automatic diagnosis of PCa from mpMRI. Each study is introduced and described briefly in the following chapter and in more detail in the individual manuscripts in the appendix.

5.1. STUDY 1: PAPER A

Title: Computer Aided Detection of Prostate Cancer on Biparametric MRI Using a Quadratic Discriminant Model

5.1.1. INTRODUCTION

Transrectal ultrasound guided biopsies (TRUS+B) is the current standard technique for prostate cancer (PCa) diagnosis. TRUS+B, however, lacks in both sensitivity and specificity for PCa detection and staging. Because most PCa lesions are not visible on ultrasound, 10-12 biopsies are obtained systematically, but randomly, from the peripheral zone of the gland. This approach has a risk of missing significant lesions, or not hitting the most aggressive part of the lesion with the biopsy needle. Conversely, insignificant lesions may be hit, thereby leading to over detection and risk of overtreatment.

Multiparametric MRI (mpMRI) guided biopsies have been found to improve the detection of clinically significant tumours and decrease detection of insignificant tumours compared to TRUS+B. Furthermore, it helps reduce the number of unnecessary biopsies and gives a better assessment of the cancer aggressiveness. Because PCa screening of MRI is labour-intensive, requires high level of expertise and is affected by inter-observer variation, semi-or fully automatic methods are increasingly being investigated for the purpose. Computerised methods have the potential of reducing reading time and variation between observers, and at the same time improve the detection of clinically significant PCa lesions.

This study presents an algorithm for detection of PCa in the whole prostate gland using MRI based on T2W and DWI (and ADC) imaging sequences and comparison to expert annotations.

5.1.2. METHODS

A dataset consisting of 18 patients (with 22 lesions) diagnosed with local or locally advanced PCa was used for this study, together with expert delineation of the prostate gland and PCa lesion on T2W. Image features were extracted from each voxel in T2W, DWI and ADC image sequence and used for classifying voxels as either cancerous or non-cancerous. Extracted features were: Intensity, 3d image gradient magnitude and direction. Also, a distance feature (Euclidean) measuring distance from the prostate boundary to each voxel was used.

Classification was done using a quadratic discriminant model (QDA) in a leave-one-out cross-validation setup.

5.1.3. MAIN RESULTS

The algorithm detected 21 out of 22 tumours with median of 1 false positive per patient. Figure 9 shows some examples of the classifier output prediction map from 4 different patients.

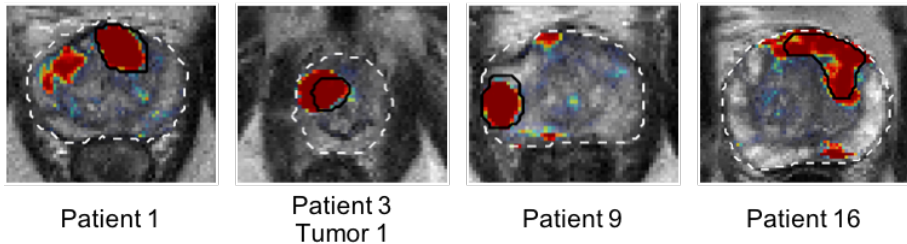Patient 1   Patient 3 Tumor 1   Patient 9   Patient 16

Figure 9. Example probability maps (0 probability is transparent) overlaid T2W for 4 patients from Paper A. Modified from [149]*.*

An AUC of 0.83 was obtained which is comparable to performances reported by others (AUC range 0.8-0.89).

The study is described in detail in Paper A.

5.2. STUDY 2: PAPER B

Title: Assessment of Prostate Cancer Prognostic Gleason Grade Group using Zonal Specific Features Extracted from Biparametric MRI – a Machine Learning Approach

5.2.1. INTRODUCTION

Prostate cancer (PCa) ranges from a nonsignificant indolent to an aggressive cancer with fatal outcome. The aggressiveness is graded by the Gleason Score (GS), which is a powerful predictor of progression, mortality, and the outcome of the disease. A higher GS indicates a higher level of aggression with a worse prognosis. The GS is found from prostate biopsies and used for clinical decision making, selection of treatment and prediction of the outcome.

The GS from the biopsies often differs from that determined after radical prostatectomy (surgical removal of the prostate) due to the random sampling when obtaining the biopsies.

The ability to distinguish indolent, intermediate, and aggressive PCa is limited at the time of diagnosis, leading to incorrect risk stratification and possible over- and under treatment.

Several studies suggest that MRI has the ability to non-invasively assess the GS and could be used in the treatment planning. As the analysis of prostate MRI is time-consuming, complex and affected by interobserver variability, automatic methods are increasingly being designed to assist radiologists and could overcome the before-mentioned limitations.

Current studies predominantly classified PCa lesions into two classes (malignant from non-malignant lesions, or indolent/low grade (GS=3+3) from clinically significant/high grade (GS≥3+4)). Additionally, the majority of the current studies are limited to only one zone of the prostate, often the peripheral zone (PZ), which is not optimal as the disease also occurs in other prostatic zones.

This study presents an algorithm for accurate determination of the GS (into four classes) of PCa lesions from the whole prostate gland using zonal specific image features from either T2W or DWI MRI images.

5.2.2. METHODS

Image and patient data used for this study were obtained from The Cancer Imaging Archive (TCIA). MRI examinations included axial T2W and DWI sequences from 99 patients, with a total of 112 lesions, scanned on two different 3T Siemens scanners. For each lesion the zonal location and centre coordinate were provided together with the pathological-defined Prognostic Gleason Grade Group (GG), split into GG 1 (GS = 6), GG 2 (GS 3+4=7), GG 3 (GS 4+3=7), GG 4 (GS = 8) and GG 5 (GS = 9-10). As preprocessing, the images were resampled to 0.5mm x 0.5mm, and the T2W images were z-score normalised to account for variation in intensity between patients. A region of interest (ROI) was defined as a 61x61 voxel around the lesion centre coordinate, large enough to cover the largest lesions, but as tightly around the lesion as possible.

Texture and histogram features were extracted from the ROI in

- T2W for lesions located in the transitional zone and anterior fibromuscular stroma (TZ+AFS)
- DWI for lesions in the peripheral zone (PZ).

For selection of discriminative features, a semi-exhaustive feature search was performed using all combinations of 1-6 features from the total of 38 features extracted from each lesion. A K-Nearest Neighbour classifier with feature normalisation and correlation as distance measure was used to evaluate each feature combination in a stratified 3-fold cross validation setup using AUC (Receiver Operator Characteristic area under curve) as measure.

The following binary models were analysed:

- GG1 versus GG2-5
- GG2 versus GG1+3+4+5
- GG1+2 versus GG3-5
- GG3 versus GG1+2+4+5
- GG4+5 versus GG1-3

5.2.3. MAIN RESULTS

The main results from this study is presented in Table 2 for all the binary models.

Table 2. Main results from Paper B. PZ = Peripheral Zone. TZ+AFS = Transition Zone and Anterior Fibromuscular Stroma

Models	AUC PZ	AUC TZ+AFS
GG1 versus GG2-5	0.8722	0.8473
GG2 versus G1+3+4+5	0.8839	0.8929
GG1+2 versus GG3-5	0.9571	0.8254
GG3 versus GG1+2+4+5	0.9762	0.9387
GG4+5 versus GG1-3	0.9056	0.8711

A combination of histogram and texture features was found to give the best performing classifier. Five to six features were used from the DWI imaging sequence for the PZ and four to six features from T2W imaging for TZ+AFS.

The study is thoroughly described in Paper B

5.3. STUDY 3: PAPER C

Title: Prostate Zonal Segmentation in 1.5T and 3T T2W MRI using a Convolutional Neural Network

5.3.1. INTRODUCTION

A segmentation of the prostate gland from its surrounding tissues is essential for several clinical tasks such as; determination of volume, systems for MRI/ultrasound fusion for guided biopsies, PI-RADS lesion detection and scoring, target delineation for radiotherapy treatment, or to obtain the region of interest for computer-aided diagnosis systems. A manual delineation of the prostate from MR images is a labour-intensive task with high risk of inter- and intra-observer variability. Automatic algorithms for prostate segmentation have been an active research field for several years as they greatly enhance the clinical workflow and reduce the subjectivity.

Recently, a greater part of research has focused on zonal segmentation of the prostate into central gland (CG) and peripheral zone (PZ). Because the majority of prostate cancers (PCas) are located in the PZ, a precise zonal location of the lesion is extremely important and favours the treatment outcome. Also, PCa lesions located in the PZ tend to have higher Gleason score and have significantly different biological behaviour and could therefore be candidates for a more aggressive treatment.

Literature on automatic methods for zonal segmentation of the prostate is relatively sparse. Previously published studies on the subject only included images obtained from one scanner or obtained dice score coefficient (DSC) values inadequate for clinical purposes, especially in the proximal and distal ends of the gland. Automatic algorithms must be robust to differences in MRI acquisition protocol and magnetic field strength of the MRI scanner and perform equally well over the entire organ.

Convolutional neural networks (CNNs) have shown great success in automatic medical image segmentation achieving state-of-the-art performances. This study proposes an algorithm for zonal segmentation of the prostate using T2W MRI on prostate examinations from two different scanners (GE 1.5T (scanned with endorectal coil (ERC)) and Siemens 3T) using a CNN.

5.3.2. METHODS

A publicly available dataset was used for this study, consisting of 40 patients with elevated PSA level, six PCa negative and 34 PCa positive with varying lesion size and location. The patients were MRI scanned on two different scanners; 21 patients on a

General Electric (GE) 1.5T scanner with ERC, and 19 patients on a Siemens 3T scanner. The MRI examination consisted of a T2W imaging sequence together with one or more functional sequences. An experienced radiologist delineated the CG and PZ, which served as the ground truth (GT).

Images were resampled to 0.5x0.5x0.5 mm voxels, using bicubic interpolation, to account for differences in voxel spacing and slice thickness, and z-score normalised to account for inter-patient intensity variation. As the GT was missing on some slices for the CG, these were linearly interpolated. Furthermore, the images were cropped to exclude some of the surrounding tissues, and slices not containing either CG or PZ were removed.

After preprocessing, the images were propagated through a CNN based on the U-net architecture [143]. The modifications made to the implementation of the U-net architecture for this study were: the use of zero padding to keep the output size the same as the input size and batch normalisation layers before max pooling layers in the contracting part of the network. Pixel-wise cross entropy was used as loss function with class weighting to account for class imbalance, and evaluation metric was DSC. Lastly, horizontal flip, small rotations, width and height shift, zoom and shearing were used as data augmentation during training.

Stratified (according to scanner) 5-fold cross-validation was used for evaluation of the model, resulting in 32 patients for each training set, 8 patients for each test set. Two patients (one from each scanner) were used during the training phase for validation.

5.3.3. MAIN RESULTS

Overall results from the algorithm showed:

- DSC of 0.803 for CG and 0.684 for PZ.
- The mid-gland showed significantly higher DSC compared to apex and base for both zones.
- No significant difference in DSC between the two scanners.

An example of zonal segmentation from one patient is shown in Figure 10. This patient achieved DSC of 0.968 and 0.905 for CG and PZ, respectively.
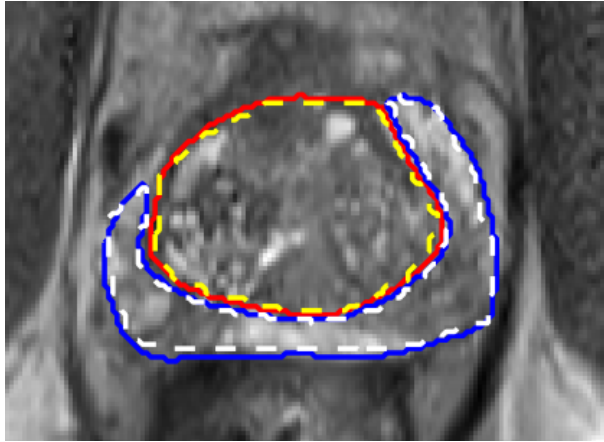
Figure 10. Zonal segmentation result from patient 32 scanned on 3T Siemens scanner, slice no. 32. Red solid line = segmentation CG, yellow dashed line = ground truth CG, blue solid line = segmentation PZ and white dashed line = ground truth PZ.

The results of this study are promising and have clinical potential. The DSC are comparable to the current literature on zonal segmentation.

A full description of the study is presented in Paper C.

CHAPTER 6. DISCUSSION AND CONCLUSIONS

The following chapter presents an overall discussion of the PhD work. At the end of the chapter, suggestions for future work will be presented together with a conclusion of the work. A specific discussion and conclusion for each of the three studies can be found in the papers (**Paper A, B and C**).

6.1. DISCUSSION

The aim of this PhD work was to investigate automatic methods for prostate cancer (PCa) diagnosis on mpMRI. Three studies were carried out during the course of this PhD work with the first focusing on automatic detection of PCa from mpMRI. The second study aiming at assessing PCa aggressiveness from imaging features from mpMRI and lastly, study three, investigating automatic zonal segmentation of the prostate gland.

In the first study (**Paper A**) it was shown that automatic detection of PCa from mpMRI is can be attained, with reasonable performance, detecting 21 out of 22 PCa lesions in the 18 patients. At the time of the first study, the focus in the literature was to demonstrate the feasibility of automatic detection of PCa on mpMRI and identify sequences and features of interest. Since then, the published papers have focused more on classification of predefined lesions as either malignant or benign [150]. This might be due to the great improvement of human readers in finding clinically significant PCa lesions after the introduction of the PI-RADS scoring system compared to the traditional diagnostic technique (TRUS+B). The remaining problem then is, that even though the sensitivity for radiologists is very high (near perfect), the specificity is low (around 30%). This means that the radiologists find nearly all cancers, however, a large part of the lesions that the radiologist suspects to be significant cancer, turns out to be non-cancerous tissue on pathology. This sets a demand for automatic algorithms for removing false positive lesions (i.e. not-clinically significant or benign lesions). Combining radiologist with an automatic classification algorithm can result in much higher specificity, while preserving the high sensitivity [151].

To resolve this challenge, the SPIE-AAPM-NCI Prostate MR Classification Challenge was announced in 2016. The aim of the challenge was to differentiate between clinically significant and clinically insignificant lesions from a data set consisting of 346 patients. The challenge is still ongoing, but the winning group in 2017 obtaining AUC of 0.87 with two running up at AUC of 0.84 [123].

Later came a new challenge (ProstateX-2, running from May 2017 to June 2017) within classification of prostate lesions from mpMRI, now all clinically significant, with the goal of classifying them into their respective Gleason grade group. The full dataset consists of 162 mpMRI cases with location and pathology-defined Gleason grade group of each lesion. The training data from this challenge were used for study two (**Paper B**) for classification of lesions into their respective Gleason grade groups. The results were promising, however, as the test set has not yet been released, validation of the algorithm on an independent dataset is still warranted.

For both study one and two (**Paper A and B**), it was chosen to use bpMRI (T2W and DWI (including ADC)) imaging for the analysis since DCE has several disadvantages like long scan-time and use of expensive contrast agent (as described in section 2.2.1). Studies have shown non-inferior performance of bpMRI to mpMRI of human readers [82,152]. Furthermore, the use of expensive contrast agent, with risk of allergic reaction, could be avoided. The DCE sequence only plays a minor role in the newest version of PI-RADS (v2), and it has been suggested to remove the sequence in later versions of the guidelines [153]. Therefore, using only bpMRI for automatic algorithms could be of future interest to limit costs and time required for the image acquisition and might encourage greater use of MRI [83].

One of the major limitations for most of the current studies on automatic PCa diagnosis is the datasets used for the studies; data comes from one scanner with one scanning protocol, field strength, and protocol for patient preparation. This makes it difficult to compare the performance of different algorithms to each other, and, as a result, algorithms perform sub-optimally or needs adaption to new data [150,154]. As mentioned above, datasets have been made publicly available over the last few years as part of online challenges in medical image analysis, or to facilitate future discoveries from researchers within automatic algorithms [2,155]. The majority of these datasets include mpMRI examinations from different scanners (vendor, field strength etc.) which can help overcome this significant limitation in future work.

Several studies have investigated methods for automatic prostate segmentation on MRI, using a wide variety of methods, like atlas-based, active shape models, and level sets [89]. To an increasing extent, zonal segmentation of the prostate is being investigated as it is clinically meaningful for e.g. lesion detection and risk stratification. Recently, deep learning algorithms, in particular convolutional neural networks (CNN) have shown to outperform traditional machine learning approaches in a several medical imaging tasks, such as detection, classification and segmentation. The need for large amounts of labelled data limits this use in many applications [95,96,156]. The U-net architecture used in study 3 (**Paper C**) has previously been found to perform well on limited amounts of data. The CNN approach for zonal segmentation in **Paper C** showed performance comparable to the current literature, robustness to datasets from different scanners and with a relatively small dataset of 40 patients.

The exact ground truth for PCa is only available from pathological assessment of the excised prostate specimen. For patients not undergoing radical prostatectomy, this is not possible, and one must rely on the results from the biopsies and expert delineation of the area of interest. In the first study (**Paper A**), the lesions and glands were delineated by an expert. Manual delineation of the prostate is subjected to inter- and intra-observer variation, so optimally, multiple manual delineations should be used [89]. The expert had to rely on results from the biopsy report when delineating lesions, which only state part (apex, mid or base) and location (mid or lateral). That, and the fact that many of the patients only had MRI suspicious areas biopsied, could have resulted in significant lesions being missed if not clearly visible on mpMRI.

Acquiring the lesion locations directly from MRI scanner will provide a more precise ground truth compared to the one in the first study. The provided lesion locations for study two (**Paper B**) were obtained from the MRI scanner coordinates as the biopsies were obtained in the MRI scanner (in-bore MRI-guided prostate biopsy). Skipping the registration step, required for ultrasound-MRI fusion systems for guided biopsies, allows for more precise spatial locations of the obtained biopsy in MRI. There is, however, still risk of needle placement error which can result in missed cancers and incorrect Gleason score [157]. Furthermore, lesions not visible on MRI are also missed using this approach. The biopsy was obtained from the centroid of the lesion on MRI. Since PCa lesions are heterogeneous, even within same lesion, the highest Gleason score is often not located near the centre of the lesion [158]. Furthermore, there is a significant variability between pathologists when assessing the Gleason score [159]. Some studies have investigated the registration of prostate MRI and digital pathology to facilitate the use of pathology as ground truth for MRI analysis for determining extent and aggressiveness of the PCa. This, however, also has several limitations, especially the deformation of the excised prostate specimen, errors introduced during slicing, quarter mount step-sectioning and later pseudo whole mount assembly [160–163].

The general framework for automatic PCa diagnosis system includes image registration. No registration was done in study one (**Paper A**), except for using coordinates from scanner. Using bpMRI compared to mpMRI decreases the risk of patient movement and thereby the need for registration. However, spatial mismatch between the imaging sequences could affect the performance. To account for this, study one (**Paper A**) focused solely on detection and not segmentation of the lesions, so that there is a good possibility that the lesion will overlap to some degree on T2W and DWI. The study did show tendency to underestimate the tumour area, which could be explained by spatial mismatch.

Paradigm Shift in Prostate Cancer Diagnosis

Concurrently to the PhD studies, a lot have changed in the diagnostic pathway of PCa patients. The use of mpMRI for the diagnosis has shifted from being a promising

method for improving the diagnosis, especially for targeted repeat biopsy in patients with persistent clinical suspicion, to a pivotal tool in the clinical guidelines for staging, treatment planning (patients suited for active surveillance, nerve sparing surgery and for predicting positive surgical margins), risk assessment and in detecting local recurrences [164]. Currently, the use of mpMRI as triage test for patients with suspicion of PCa is under investigation due to mpMRI high reliability in excluding clinically significant PCa [71].

Increasing use of mpMRI for PCa diagnosis increases the requirement for radiologists to meet additional clinical demands of the second most common cancer in males. Major limitation of using mpMRI for PCa diagnosis is the interobserver variability, time consumption, complexity and heterogeneity in the scoring criteria [46,165]. In these cases, automatic methods can be of great value, but it is still a young field of research with different challenges to be solved [2]. A complete system should include all aspects (preprocessing (possibly including registration), segmentation, detection and classification) and all zones of the gland to become applicable in a clinical environment. Overall goal of such a system is not to replace the clinician but rather to ease the workflow and aid in the diagnosis and risk stratification.

Recently, an automatic tool for mpMRI PCa analysis was commercialised (Watson Elementary, Watson Medical, Den Ham, The Netherlands). The software performs registration between MRI sequences, extracts features from all imaging sequences and assigns a malignancy score to every voxel thereby highlighting suspect lesions. Studies validating Watson Elementary have, however, shown contradictory results. One study found the performance of Watson Elementary comparable to two board-certified radiologists (based on first version of the PI-RADS scoring system) [166]. Another study found an insufficient performance of the system based data from their hospital database and suggested that the performance of the system might be dataset dependent (e.g. different imaging acquisition configurations). They concluded that the system does not qualify for PCa detection and prediction of aggressiveness [8].

So far, no commercialised full system has shown sufficient performance for clinical application which suggest that more work on the subject is warranted, preferably on a broader pool of multicentre datasets to improve the general applicability of automatic algorithms for PCa diagnosis [87].

6.2. FUTURE PERSPECTIVES

Over the course of this PhD work there has been a notable shift from using traditional machine learning to deep learning based approaches. A clear advantage of deep learning approaches is that the imaging features are automatically extracted by the network which is often a difficult and tedious task for the scientist. In future work it could be interesting to compare the results of the classifiers in **Paper A** and **Paper B** with deep learning approaches.

Many applications within PCa diagnosis from MRI are still not fully explored in the literature. Automatic lesion detection and segmentation from MRI for e.g. image guided interventions could be explored for radiotherapy planning. The use of MRI as the sole modality for radiotherapy planning is an area of growing scientific interest, and is especially interesting in soft tissue organs where MRI has superior contrast compared to computed tomography (CT) [167].

Active surveillance (AS) is increasingly being used for low-risk PCa management with patients being closely followed to detect patients who convert to higher cancer grade. mpMRI has already showed excellent performance in risk stratification of PCa patients compared to current standard TRUS+B. Therefore, mpMRI is an excellent choice for identifying patients for AS. Using mpMRI to monitor progression in these patients instead of repeat biopsies could be an attractive future application of mpMRI. However, at present, there is not enough evidence supporting this. Finding imaging biomarkers that can safely predict which patients are suitable for AS will be of great value for low-risk patients resulting in reducing unnecessary radical treatment [43].

MRI has proven useful as biomarker for detection of biochemical recurrence [168]. Using pre-treatment MRI as predictor of who will have disease recurrence could serve as a valuable tool for selecting patients for more aggressive treatment and closer follow-up. Such a study requires a large number of patients with MRI examination followed over a long period of time, to be able to include a sufficient number of patients who have recurrence.

6.3. CONCLUSION

This PhD thesis begins by introducing the challenges related to the diagnosis in prostate cancer, and particularly in relation to the use of mpMRI for the diagnosis. These challenges gave rise to the research motivation of this work.

The first objective of the thesis was to automatically detect PCa lesions from MRI. This was achieved in **Paper A** with performance comparable to the literature with a low number of false positives using imaging features from T2W and DWI (+ADC) imaging sequences.

Second objective was to classify PCa lesions into levels of aggression based on MRI features which was answered in **Paper B** with results showing clinical potential that warrant further investigation.

Last study (**Paper C**) investigated the use of a deep learning-based approach for zonal segmentation of the prostate. This study showed promising results with some patients showing segmentations very close to the expert delineation. As other studies in the literature, the performance was better in the mid-gland compared to the apex and base.

Overall the work has shown that it is possible to develop automatic algorithms for PCa analysis on mpMRI with reasonable results, more precisely detection of PCa lesions, classification of PCa lesions and zonal segmentation of the gland.

REFERENCES

[1]   Litjens G, Debats O, Barentsz J, Karssemeijer N, Huisman H. Computer-aided detection of prostate cancer in MRI. IEEE Trans Med Imaging 2014;33:1083–92. doi:10.1109/TMI.2014.2303821.

[2]   Lemaître G, Martí R, Freixenet J, Vilanova JC, Walker PM, Meriaudeau F. Computer-Aided Detection and diagnosis for prostate cancer based on mono and multi-parametric MRI: A review. Comput Biol Med 2015;60:8–31. doi:10.1016/j.compbiomed.2015.02.009.

[3]   Wallace TJ, Torre T, Grob M, Yu J, Avital I, Brücher B, et al. Current Approaches, Challenges and Future Directions for Monitoring Treatment Response in Prostate Cancer. J Cancer 2014;5:3–24. doi:10.7150/jca.7709.

[4]   De Rooij M, Hamoen EHJ, Fütterer JJ, Barentsz JO, Rovers MM. Accuracy of multiparametric MRI for prostate cancer detection: A meta-analysis. Am J Roentgenol 2014;202:343–51. doi:10.2214/AJR.13.11046.

[5]   Reisæter LAR, Fütterer JJ, Losnegård A, Nygård Y, Monssen J, Gravdal K, et al. Optimising preoperative risk stratification tools for prostate cancer using mpMRI. Eur Radiol 2018;28:1016–26. doi:10.1007/s00330-017-5031-5.

[6]   Hamdy FC, Lamb AD, Bryant RJ. Diagnostic Pathways for Screen-detected Prostate Cancer: The Plot Thickens. Eur Urol 2018;73:351–2. doi:10.1016/j.eururo.2017.11.011.

[7]   Vilanova JC, Catalá V, Algaba F, Laucirica Editors O. Atlas of Multiparametric Prostate MRI: With PI-RADS Approach and Anatomic-MRI-Pathological Correlation. Springer; 2017. doi:https://doi-org.zorac.aub.aau.dk/10.1007/978-3-319-61786-2.

[8]   Thon A, Teichgräber U, Tennstedt-Schenk C, Hadjidemetriou S, Winzler S, Malich A, et al. Computer aided detection in prostate cancer diagnostics: A promising alternative to biopsy? A retrospective study from 104 lesions with histological ground truth. PLoS One 2017;12. doi:10.1371/journal.pone.0185995.

[9]   Hoeks CMA, Barentsz JO, Hambrock T, Yakar D, Somford DM, Heijmink SWTPJ, et al. Prostate cancer: multiparametric MR imaging for detection, localization, and staging. Radiology 2011;261:46–66.

doi:10.1148/radiol.11091822.

[10]   Pokorny MR, De Rooij M, Duncan E, Schröder FH, Parkinson R, Barentsz
        JO, et al. Prospective Study of Diagnostic Accuracy Comparing Prostate
        Cancer Detection by Transrectal Ultrasound-Guided Biopsy Versus
        Magnetic Resonance (MR) Imaging with Subsequent MR-guided Biopsy in
        Men Without Previous Prostate Biopsies. Eur Urol 2014;66:22–9.
        doi:10.1016/j.eururo.2014.03.002.

[11]   Liu L, Tian Z, Zhang Z, Fei B. Computer-aided Detection of Prostate
        Cancer with MRI: Technology and Applications. Acad Radiol
        2016;23:1024–46. doi:10.1016/j.acra.2016.03.010.

[12]   Litjens GJS, Vos PC, Barentsz JO, Karssemeijer N, Huisman HJ. Automatic
        computer aided detection of abnormalities in multi-parametric prostate MRI.
        Med. Imaging 2011 Comput. Diagnosis, vol. 7963, 2011, p. 79630T.
        doi:10.1117/12.877844.

[13]   Siegel RL, Miller KD, Jemal A, Data M. Cancer Statistics, 2016. CA Cancer
        J Clin 2016;66:7–30. doi:10.3322/caac.21332.

[14]   National Collaborating Centre for Cancer. Prostate Cancer: diagnosis and
        treatment. Clinical guideline. Natl Inst Heal Care Excell 2014:1–480.

[15]   American Cancer Society. Key statistics for prostate cancer 2016.
        https://www.cancer.org/cancer/prostate-cancer/about/key-statistics.html
        (accessed August 20, 2018).

[16]   Tchrakian N, Cotter MB, Loda M. Pathology and molecular pathology of
        prostate cancer. Pathol. Epidemiol. Cancer, Cham: Springer International
        Publishing; 2016, p. 127–49. doi:10.1007/978-3-319-35153-7_10.

[17]   Fütterer JJ, Barentsz JO. 3T MRI of prostate cancer. Appl Radiol
        2009;38:25.

[18]   Shariat SF, Roehrborn CG. Using biopsy to detect prostate cancer. Rev Urol
        2008;10:262–80.

[19]   Hoogland a. M, Kweldam CF, Leenders GJLH Van, van Leenders GJLH.
        Prognostic Histopathological and Molecular Markers on Prostate Cancer
        Needle-Biopsies: A Review. Biomed Res Int 2014;2014:1–12.
        doi:10.1155/2014/341324.

[20]   Thompson IM, Pauler DK, Goodman PJ, Tangen CM, Lucia MS, Parnes

HL, et al. Prevalence of Prostate Cancer among Men with a Prostate -
Specific Antigen Level 4.0 ng per Milliliter or less. N Engl J Med
2004;350:2239–46.

[21] Saini S. PSA and beyond: alternative prostate cancer biomarkers. Cell Oncol
2016;39:97–106. doi:10.1007/s13402-016-0268-6.

[22] D'Amico A V, Chen M-H, Roehl KA, Catalona WJ. Preoperative PSA
velocity and the risk of death from prostate cancer after radical
prostatectomy. N Engl J Med 2004;351:125–35.
doi:10.1056/NEJMoa032975.

[23] Mottet N, Bellmunt J, Briers E, Bolla M, Cornford P, De Santis M, et al.
EAU-ESTRO-SIOG Guidelines on Prostate Cancer 2016:1–146.
http://uroweb.org/guideline/prostate-cancer/ (accessed September 7, 2016).

[24] Sumura M, Shigeno K, Hyuga T, Yoneda T, Shiina H, Igawa M. Initial
evaluation of prostate cancer with real-time elastography based on step-
section pathologic analysis after radical prostatectomy: A preliminary study.
Int J Urol 2007;14:811–6. doi:10.1111/j.1442-2042.2007.01829.x.

[25] Hwang SI, Lee HJ. The future perspectives in transrectal prostate ultrasound
guided biopsy. Prostate Int 2014;2:153–60. doi:10.12954/PI.14062.

[26] Boesen L, Noergaard N, Chabanova E, Logager V, Balslev I, Mikines K, et
al. Early experience with multiparametric magnetic resonance imaging-
targeted biopsies under visual transrectal ultrasound guidance in patients
suspicious for prostate cancer undergoing repeated biopsy. Scand J Urol
2015;49:25–34. doi:10.3109/21681805.2014.925497.

[27] Ploussard G, Nicolaiew N, Marchand C, Terry S, Allory Y, Vacherot F, et
al. Risk of repeat biopsy and prostate cancer detection after an initial
extended negative biopsy: Longitudinal follow-up from a prospective trial.
BJU Int 2013;111:988–96. doi:10.1111/j.1464-410X.2012.11607.x.

[28] Boesen L. Multiparametric MRI in detection and staging of prostate cancer.
Dan Med J 2017;64.

[29] Institute NC. Definition of transrectal biopsy - NCI Dictionary of Cancer
Terms n.d. https://www.cancer.gov/publications/dictionaries/cancer-
terms/def/transrectal-biopsy (accessed September 7, 2018).

[30] Gordetsky J, Epstein J. Grading of prostatic adenocarcinoma: current state
and prognostic implications. Diagn Pathol 2016;11:25. doi:10.1186/s13000-

016-0478-2.

[31]   Sfoungaristos S, Perimenis P. Clinical and pathological variables that predict changes in tumour grade after radical prostatectomy in patients with prostate cancer. Can Urol Assoc J 2013;7:E93-97. doi:10.5489/cuaj.270.

[32]   Epstein JI, Egevad L, Amin MB, Delahunt B, Srigley JR, Humphrey PA, et al. The 2014 International Society of Urological Pathology (ISUP) Consensus Conference on Gleason Grading of Prostatic Carcinoma: Definition of Grading Patterns and Proposal for a New Grading System. Am J Surg Pathol 2016;40:244–52. doi:10.1097/PAS.0000000000000530.

[33]   Chen N, Zhou Q. The evolving Gleason grading system. Chinese J Cancer Res 2016;28:58–64. doi:10.3978/j.issn.1000-9604.2016.02.04.

[34]   Gleason DF, Mellinger GT, Arduino LJ, Bailar JC, Becker LE, Berman HI, et al. Prediction of Prognosis for Prostatic Adenocarcinoma by Combined Histological Grading and Clinical Staging. J Urol 1974;111:58–64. doi:10.1016/S0022-5347(17)59889-4.

[35]   Epstein JI, Zelefsky MJ, Sjoberg DD, Nelson JB, Egevad L, Magi-Galluzzi C, et al. A Contemporary Prostate Cancer Grading System: A Validated Alternative to the Gleason Score. Eur Urol 2016;69:428–35. doi:10.1016/j.eururo.2015.06.046.

[36]   Lavery HJ, Cooperberg MR. Clinically localized prostate cancer in 2017: A review of comparative effectiveness. Urol Oncol 2017;35:40–1. doi:10.1016/j.urolonc.2016.11.013.

[37]   Incrocci L. Radiotherapy for prostate cancer and sexual health. Transl Androl Urol 2015;4:124–30. doi:10.3978/j.issn.2223-4683.2014.12.08.

[38]   Bolla M. Treatment of localized or locally advanced prostate cancer: The clinical use of radiotherapy. EAU Updat Ser 2003;1:23–31. doi:10.1016/S1570-9124(03)00006-0.

[39]   Washington CM, Leaver DT. Principles and Practice of Radiation Therapy. Elsevier Health Sciences; 2015.

[40]   Nam RK, Cheung P, Herschorn S, Saskin R, Su J, Klotz LH, et al. Incidence of complications other than urinary incontinence or erectile dysfunction after radical prostatectomy or radiotherapy for prostate cancer : a population-based cohort study. Lancet Oncol 2014;15:223–31. doi:10.1016/S1470-2045(13)70606-5.

[41]   Eggener SE, Badani K, Barocas DA, Barrisford GW, Cheng JS, Chin AI, et al. Gleason 6 prostate cancer: Translating biology into population health. J Urol 2015;194:626–34. doi:10.1016/j.juro.2015.01.126.

[42]   Klotz L. Prostate cancer overdiagnosis and overtreatment. Curr Opin Endocrinol Diabetes Obes 2013;20:204–9. doi:10.1097/MED.0b013e328360332a.

[43]   Choyke PL, Loeb S. Active Surveillance of Prostate Cancer. Oncology (Williston Park) 2017;31:67–70.

[44]   Silberstein JL, Pal SK, Lewis B, Sartor O. Current clinical challenges in prostate cancer. Transl Androl Urol 2013;2:122–36. doi:10.3978/j.issn.2223-4683.2013.09.03.

[45]   Padhani AR, Weinreb J, Rosenkrantsz AB, Villeirs G, Turkbey B, Barentsz J. Prostate Imaging-Reporting and Data System Steering Committee: PI-RADS v2 Status Update and Future Directions. Eur Urol 2018. doi:10.1016/j.eururo.2018.05.035.

[46]   Mottet N, Bellmunt J, Bolla M, Briers E, Cumberbatch MG, De Santis M, et al. EAU-ESTRO-SIOG Guidelines on Prostate Cancer. Part 1: Screening, Diagnosis, and Local Treatment with Curative Intent. Eur Urol 2017;71:618–29. doi:10.1016/j.eururo.2016.08.003.

[47]   Kasivisvanathan V, Rannikko AS, Borghi M, Panebianco V, Mynderse LA, Vaarala MH, et al. MRI-Targeted or Standard Biopsy for Prostate-Cancer Diagnosis. N Engl J Med 2018;378:1767–77. doi:10.1056/NEJMoa1801993.

[48]   Mayor S. MRI increases detection of prostate cancers and reduces overdiagnosis, finds study. Br Med J 2018;360. doi:10.1056/NEJMoa1801993.

[49]   Gaunay GS, Patel V, Shah P, Moreira D, Rastinehad AR, Ben-Levi E, et al. Multi-parametric MRI of the prostate: Factors predicting extracapsular extension at the time of radical prostatectomy. Asian J Urol 2017;4:31–6. doi:10.1016/j.ajur.2016.07.002.

[50]   Milonas D, Kinčius M, Skulčius G, Matjošaitis AJ, Gudinavičiene I, Jievaltas M. Evaluation of D'Amico criteria for low-risk prostate cancer. Scand J Urol 2014;48:344–9. doi:10.3109/21681805.2013.870602.

[51]   Feng TS, Reza Sharif-Afshar A, Wu J, Li Q, Luthringer D, Saouaf R, et al. Multiparametric MRI Improves Accuracy of Clinical Nomograms for

Predicting Extracapsular Extension of Prostate Cancer. Urology 2015;86:332–7. doi:10.1016/j.urology.2015.06.003.

[52]   Grivas N, Hinnen K, de Jong J, Heemsbergen W, Moonen L, Witteveen T, et al. Seminal vesicle invasion on multi-parametric magnetic resonance imaging: Correlation with histopathology. Eur J Radiol 2018;98:107–12. doi:10.1016/j.ejrad.2017.11.013.

[53]   Pedler K, Kitzing YX, Varol C, Arianayagam M. The current status of MRI in prostate cancer. Aust Fam Physician 2015;44:225.

[54]   Epstein JI, Feng Z, Trock BJ, Pierorazio PM. Upgrading and Downgrading of Prostate Cancer from Biopsy to Radical Prostatectomy: Incidence and Predictive Factors Using the Modified Gleason Grading System and Factoring in Tertiary Grades. Eur Urol 2012;61:1019–24. doi:10.1016/j.eururo.2012.01.050.

[55]   Shaish H, Kang SK, Rosenkrantz AB. The utility of quantitative ADC values for differentiating high-risk from low-risk prostate cancer: a systematic review and meta-analysis. Abdom Radiol 2017;42:260–70. doi:10.1007/s00261-016-0848-y.

[56]   Donati OF, Mazaheri Y, Afaq A, Vargas HA, Zheng J, Moskowitz CS, et al. Prostate Cancer Aggressiveness: Assessment with Whole-Lesion Histogram Analysis of the Apparent Diffusion Coefficient. Radiology 2014;271. doi:10.1148/radiol.13130973.

[57]   Kim TH, Kim CK, Park BK, Jeon HG, Jeong BC, Seo S Il, et al. Relationship between Gleason score and apparent diffusion coefficients of diffusion-weighted magnetic resonance imaging in prostate cancer patients. Can Urol Assoc J 2016;10:E377–82. doi:10.5489/cuaj.3896.

[58]   Knoedler JJ, Karnes RJ, Thompson RH, Rangel LJ, Bergstralh EJ, Boorjian SA. The association of tumor volume with mortality following radical prostatectomy. Prostate Cancer Prostatic Dis 2014;17:144–8. doi:10.1038/pcan.2013.61.

[59]   Bratan F, Melodelima C, Souchon R, Hoang Dinh A, Mege-Lechevallier F, Crouzet S, et al. How accurate is multiparametric MR imaging in evaluation of prostate cancer volume? Radiology 2015;275:144–54. doi:10.1148/radiol.14140524.

[60]   Cornud F, Khoury G, Bouazza N, Beuvon F, Peyromaure M, Flam T, et al. Tumor target volume for focal therapy of prostate cancer - Does

multiparametric magnetic resonance imaging allow for a reliable estimation? J Urol 2014;191:1272–9. doi:10.1016/j.juro.2013.12.006.

[61]   Nakashima J, Tanimoto A, Imai Y, Mukai M, Horiguchi Y, Nakagawa K, et al. Endorectal MRI for prediction of tumor site, tumor size, and local extension of prostate cancer. Urology 2004;64:101–5. doi:10.1016/j.urology.2004.02.036.

[62]   Paterson NR, Lavallee LT, Nguyen LN, Witiuk K, Ross J, Mallick R, et al. Prostate volume estimations using magnetic resonance imaging and transrectal ultrasound compared to radical prostatectomy specimens. Can Urol Assoc J 2016;10:264–8. doi:10.5489/cuaj.3236.

[63]   Woodrum DA, Kawashima A, Gorny KR, Mynderse LA. Prostate cancer: state of the art imaging and focal treatment. Clin Radiol 2017;72:665–79. doi:10.1016/j.crad.2017.02.010.

[64]   Mendez MH, Joh DY, Gupta R, Polascik TJ. Current Trends and New Frontiers in Focal Therapy for Localized Prostate Cancer. Curr Urol Rep 2015;16. doi:10.1007/s11934-015-0513-y.

[65]   Barrett T, Haider MA. The Emerging Role of MRI in Prostate Cancer Active Surveillance and Ongoing Challenges. Am J Roentgenol 2017;208:131–9. doi:10.2214/AJR.16.16355.

[66]   Mertan F V, Greer MD, Borofsky S, Kabakus IM, Merino MJ, Wood BJ, et al. Multiparametric Magnetic Resonance Imaging of Recurrent Prostate Cancer. Top Magn Reson Imaging 2016;25:139–47. doi:10.1097/RMR.0000000000000088.

[67]   Panebianco V, Barchetti F, Barentsz J, Ciardi A, Cornud F, Futterer J, et al. Pitfalls in Interpreting mp-MRI of the Prostate: A Pictorial Review with Pathologic Correlation. Insights Imaging 2015;6:611–30. doi:10.1007/s13244-015-0426-9.

[68]   Rhudd A, McDonald J, Emberton M, Kasivisvanathan V. The role of the multiparametric MRI in the diagnosis of prostate cancer in biopsy-naïve men. Curr Opin Urol 2017;27:488–94. doi:10.1097/MOU.0000000000000415.

[69]   Ahmed HU, El-Shater Bosaily A, Brown LC, Gabe R, Kaplan R, Parmar MK, et al. Diagnostic accuracy of multi-parametric MRI and TRUS biopsy in prostate cancer (PROMIS): a paired validating confirmatory study. Lancet 2017;389:815–22. doi:10.1016/S0140-6736(16)32401-1.

[70]   Renard-Penna R, Roupret M, Compérat E, Rozet F, Granger B, Barkatz J, et al. Relationship between non-suspicious MRI and insignificant prostate cancer: results from a monocentric study. World J Urol 2016;34:673–8. doi:10.1007/s00345-015-1685-2.

[71]   Panebianco V, Barchetti G, Simone G, Del Monte M, Ciardi A, Grompone MD, et al. Negative Multiparametric Magnetic Resonance Imaging for Prostate Cancer: What's Next? Eur Urol 2018;74:48–54. doi:10.1016/j.eururo.2018.03.007.

[72]   De Visschere P. Improving the Diagnosis of Clinically Significant Prostate Cancer with Magnetic Resonance Imaging. J Belgian Soc Radiol 2018;102:1–8. doi:10.5334/jbsr.1438.

[73]   Kim Y, Hsu ICJ, Pouliot J, Noworolski SM, Vigneron DB, Kurhanewicz J. Expandable and rigid endorectal coils for prostate MRI: Impact on prostate distortion and rigid image registration. Med Phys 2005;32:3569–78. doi:10.1118/1.2122467.

[74]   Weinreb JC, Barentsz JO, Choyke PL, Cornud F, Haider MA, Macura KJ, et al. PI-RADS Prostate Imaging - Reporting and Data System: 2015, Version 2. Eur Urol 2015;69:16–40. doi:10.1016/j.eururo.2015.08.052.

[75]   Wang L, Mazaheri Y, Zhang J, Ishill NM, Kuroiwa K, Hricak H. Assessment of Biologic Aggressiveness of Prostate Cancer: Correlation of MR Signal Intensity with Gleason Grade after Radical Prostatectomy. Radiology 2008;246:168–76. doi:10.1148/radiol.2461070057.

[76]   Sankineni S, Osman M, Choyke PL. Functional MRI in prostate cancer detection. Biomed Res Int 2014;2014. doi:10.1155/2014/590638.

[77]   Low RN, Fuller DB, Muradyan N. Dynamic gadolinium-enhanced perfusion MRI of prostate cancer: Assessment of response to hypofractionated robotic stereotactic body radiation therapy. Am J Roentgenol 2011;197:907–15. doi:10.2214/AJR.10.6356.

[78]   Lee DJ, Ahmed HU, Moore CM, Emberton M, Ehdaie B. Multiparametric magnetic resonance imaging in the management and diagnosis of prostate cancer: current applications and strategies. Curr Urol Rep 2014;15:390. doi:10.1007/s11934-013-0390-1.

[79]   Türkbey B, Thomasson D, Pang Y, Bernardo M, Choyke PL. The role of dynamic contrast-enhanced MRI in cancer diagnosis and treatment. Diagnostic Interv Radiol 2010;16:186–92. doi:10.4261/1305-

3825.DIR.2537-08.1.

[80]   Notley M, Yu J, Fulcher AS, Turner MA, Cockrell CH, Nguyen D.
         Diagnosis of recurrent prostate cancer and its mimics at multiparametric
         prostate MRI. Br J Radiol 2015;88. doi:10.1259/bjr.20150362.

[81]   Boesen L, Nørgaard N, Løgager V, Balslev I, Bisbjerg R, Thestrup K-C, et
         al. Assessment of the Diagnostic Accuracy of Biparametric Magnetic
         Resonance Imaging for Prostate Cancer in Biopsy-Naive Men. JAMA Netw
         Open 2018;1:e180219. doi:10.1001/jamanetworkopen.2018.0219.

[82]   Cecilie K, Thestrup D, Logager V, Baslev I, Møller JMM, Hansen RHH, et
         al. Biparametric versus multiparametric MRI in the diagnosis of prostate
         cancer. Acta Radiol Open 2016;5:2058460116663046.
         doi:10.1177/2058460116663046.

[83]   Jambor I, Boström PJ, Taimen P, Syvänen K, Kähkönen E, Kallajoki M, et
         al. Novel biparametric MRI and targeted biopsy improves risk stratification
         in men with a clinical suspicion of prostate cancer (IMPROD Trial). J Magn
         Reson Imaging 2017;46:1089–95. doi:10.1002/jmri.25641.

[84]   Gupta RT, Rosenkrantz AB. Prostate MRI can be accurate but can
         variability be reduced? Nat Rev Urol 2018;15:339–40. doi:10.1038/s41585-
         018-0002-4.

[85]   Walz J. The "PROMIS" of Magnetic Resonance Imaging Cost Effectiveness
         in Prostate Cancer Diagnosis? Eur Urol 2018;73:31–2.
         doi:10.1016/j.eururo.2017.09.015.

[86]   Hambrock T, Vos PC, Kaa CAH de, Barentsz JO, Huisman HJ. Prostate
         cancer: Computer-aided diagnosis with multiparametric 3-T MR imaging -
         Effect on observer performance. Radiology 2013;266:521–30.
         doi:10.1148/radiol.12111634/-/DC1.

[87]   Wang S, Burtt K, Turkbey B, Choyke P, Summers RM, Wang S, et al.
         Computer Aided-Diagnosis of Prostate Cancer on Multiparametric MRI: A
         Technical Review of Current Research. Biomed Res Int 2014;2014:1–11.
         doi:10.1155/2014/789561.

[88]   Kirschner M, Jung F, Wesarg S. Automatic Prostate Segmentation in MR
         Images with a Probabilistic Active Shape Model. MICCAI Gd Chall
         Prostate MR Image Segmentation 2012.

[89]   Litjens G, Toth R, van de Ven W, Hoeks C, Kerkstra S, van Ginneken B, et

al. Evaluation of prostate segmentation algorithms for MRI: The PROMISE12 challenge. Med Image Anal 2014;18:359–73. doi:10.1016/j.media.2013.12.002.

[90]   Park SH, Gao Y, Shi Y, Shen D. Interactive prostate segmentation using atlas-guided semi-supervised learning and adaptive feature selection. Med Phys 2014;41:1–10. doi:10.1118/1.4898200.

[91]   Garg G, Juneja M. Cancer Detection with Prostate Zonal Segmentation—A Review. Proc. Int. Conf. Comput. Commun. Syst., vol. 24, Springer Singapore; 2018, p. 829–35. doi:10.1007/978-981-10-6890-4.

[92]   Li B, Patil A V., Hossack JA, Acton ST. 3D segmentation of the prostate via poisson inverse gradient initialization. Int. Conf. Image Process. ICIP, vol. 5, 2007, p. 25–8. doi:10.1109/ICIP.2007.4379756.

[93]   Palmeri ML, Miller ZA, Glass TJ, Garcia-Reyes K, Gupta RT, Rosenzweig SJ, et al. B-mode and acoustic radiation force impulse (ARFI) imaging of prostate zonal anatomy: Comparison with 3T T2-weighted MR imaging. Ultrason Imaging 2015;37:22–41. doi:10.1177/0161734614542177.

[94]   Ghose S, Oliver A, Marti R, Llado X, Vilanova J, Freixenet J, et al. A Survey of Prostate Segmentation Methodologies in Ultrasound, Magnetic Resonance and Computed Tomography Images. Comput Methods Programs Biomed 2012;108:262–87.

[95]   Shen D, Wu G, Suk H, Engineering C. Deep Learning in Medical Image Analysis. Annu Rev Biomed Eng 2017;19:221–48. doi:10.1146/annurev-bioeng-071516-044442.Deep.

[96]   Litjens G, Kooi T, Bejnordi BE, Setio AAA, Ciompi F, Ghafoorian M, et al. A survey on deep learning in medical image analysis. Med Image Anal 2017;42:60–88. doi:10.1016/j.media.2017.07.005.

[97]   Zhu Q, Du B, Turkbey B, Choyke P, Yan P. Exploiting Inter-Slice Correlation for MRI Prostate Image Segmentation, from Recursive Neural Networks Aspect. Complexity 2018;2018.

[98]   Lee JJ, Thomas IC, Nolley R, Ferrari M, Brooks JD, Leppert JT. Biologic differences between peripheral and transition zone prostate cancer. Prostate 2015;75:183–90. doi:10.1002/pros.22903.

[99]   Ehrenberg HR, Cornfeld D, Nawaf CB, Sprenkle PC, Duncan JS. Decision forests for learning prostate cancer probability maps from multiparametric

MRI. In: Tourassi GD, Armato SG, editors. Med. Imaging 2016 Comput. Diagnosis, vol. 9785, International Society for Optics and Photonics; 2016. doi:10.1117/12.2216904.

[100] Viswanath SE, Bloch NBNB, Chappelow JC, Toth R, Rofsky NM, Genega EM, et al. Central gland and peripheral zone prostate tumors have significantly different quantitative imaging signatures on 3 tesla endorectal, in vivo T2-weighted MR imagery. J Magn Reson Imaging 2012;36:213–24. doi:10.1002/jmri.23618.

[101] Vargas HA, Akin O, Franiel T, Goldman DA, Udo K, Touijer KA, et al. Normal Central Zone of the Prostate and Central Zone Involvement by Prostate Cancer: Clinical and MR Imaging Implications. Radiology 2012;262:894–902. doi:10.1148/radiol.11110663.

[102] Makni N, Iancu A, Colot O, Puech P, Mordon S, Betrouni N. Zonal segmentation of prostate using multispectral magnetic resonance images. Med Phys 2011;38:6093–105. doi:10.1118/1.3651610.

[103] Litjens G, Debats O, van de Ven W, Karssemeijer N, Huisman H. A pattern recognition approach to zonal segmentation of the prostate on MRI. Med Image Comput Comput Assist Interv 2012;15:413–20. doi:10.1007/978-3-642-33418-4_51.

[104] Toth R, Ribault J, Gentile J, Sperling D, Madabhushi A. Simultaneous segmentation of prostatic zones using Active Appearance Models with multiple coupled levelsets. Comput Vis Image Underst 2013;117:1051–60. doi:10.1016/j.cviu.2012.11.013.

[105] Chi Y, Ho H, Law YM, Tian Q, Chen HJ, Tay KJ, et al. A compact method for prostate zonal segmentation on multiparametric MRIs. Med Imaging 2014 Image-Guided Proced Robot Interv Model 2014;9036:90360N. doi:10.1117/12.2043334.

[106] Chilali O, Puech P, Lakroum S, Diaf M, Mordon S, Betrouni N. Gland and Zonal Segmentation of Prostate on T2W MR Images. J Digit Imaging 2016;29:730–6. doi:10.1007/s10278-016-9890-0.

[107] Clark T, Zhang J, Baig S, Wong A, Haider MA, Khalvati F. Fully automated segmentation of prostate whole gland and transition zone in diffusion-weighted MRI using convolutional neural networks. J Med Imaging 2017;4:1. doi:10.1117/1.JMI.4.4.041307.

[108] Zhang J, Baig S, Wong A, Haider MA, Khalvati F. A Local ROI-specific

Atlas-based Segmentation of Prostate Gland and Transitional Zone in Diffusion MRI. J Comput Vis Imaging Syst 2016;2:2–4. doi:10.15353/jcvis.v2i1.113.

[109]   Qiu W, Yuan J, Ukwatta E, Sun Y, Rajchl M, Fenster A. Dual optimization based prostate zonal segmentation in 3D MR images. Med Image Anal 2014;18:660–73. doi:10.1016/j.media.2014.02.009.

[110]   Qiu W, Yuan J, Ukwatta E, Sun Y, Rajchl M, Fenster A. Efficient 3D multi-region prostate MRI segmentation using dual optimization. Inf Process Med Imaging 2013;23:304–15.

[111]   Vikal S, Haker S, Tempany C, Fichtinger G. Prostate contouring in MRI guided biopsy. Med Imaging 2009 Image Process 2009;7259:72594A. doi:10.1117/12.812433.

[112]   Chan I, Wells W, Mulkern R V, Haker S, Zhang J, Zou KH, et al. Detection of prostate cancer by integration of line-scan diffusion, T2-mapping and T2-weighted magnetic resonance imaging; a multichannel statistical classifier. Med Phys 2003;30:2390–8. doi:10.1118/1.1593633.

[113]   Rampun A, Zheng L, Malcolm P. Computer-aided diagnosis of prostate cancer in the peripheral zone using multiparametric MRI Computer-aided detection of prostate cancer in T2-weighted MRI within the peripheral zone. Phys Med Biol 2012;57.

[114]   Peng Y, Jiang Y, Yang C, Bancroft Brown J, Tatjana Antic B, Sethi I, et al. Quantitative analysis of multiparametric prostate MR images: differentiation between prostate cancer and normal tissue and correlation with Gleason score--a computer-aided diagnosis development study. Radiology 2013;267:787–96. doi:10.1148/radiol.13121454.

[115]   Ginsburg SB, Algohary A, Pahwa S, Gulani V, Ponsky L, Aronen HJ, et al. Radiomic features for prostate cancer detection on MRI differ between the transition and peripheral zones: Preliminary findings from a multi-institutional study. J Magn Reson Imaging 2017;46:184–93. doi:10.1002/jmri.25562.

[116]   Dikaios N, Alkalbani J, Abd-Alazeez M, Sidhu HS, Kirkham A, Ahmed HU, et al. Zone-specific logistic regression models improve classification of prostate cancer on multi-parametric MRI. Eur Radiol 2015;25:2727–37. doi:10.1007/s00330-015-3636-0.

[117]   Nketiah G, Elschot M, Kim E, Teruel JR, Scheenen TW, Bathen TF, et al.

T2-weighted MRI-derived textural features reflect prostate cancer aggressiveness: preliminary results. Eur Radiol 2017;27:3050–9. doi:10.1007/s00330-016-4663-1.

[118]   Barbieri S, Brönnimann M, Boxler S, Vermathen P, Thoeny HC. Differentiation of prostate cancer lesions with high and with low Gleason score by diffusion-weighted MRI. Eur Radiol 2017;27:1547–55. doi:10.1007/s00330-016-4449-5.

[119]   Woodfield CA, Tung GA, Grand DJ, Pezzullo JA, Machan JT, Renzulli JF, et al. Diffusion-weighted MRI of peripheral zone prostate cancer: Comparison of tumor apparent diffusion coefficient with Gleason score and percentage of tumor on core biopsy. Am J Roentgenol 2010;194:W316–22. doi:10.1590/S1677-55382010000400018.

[120]   Hambrock T, Diederik M, Somford M, Huisman HJ, Van Oort IM, Witjes JA, et al. Relationship between Apparent Diffusion Coeffi cients at 3.0-T MR Imaging and Gleason Grade in Peripheral Zone Prostate Cancer 1. Radiology 2011;259:453–61. doi:10.1148/radiol.11091409.

[121]   Chen Y-JJ, Chu W-CC, Pu Y-SS, Chueh S-CC, Shun C-TT, Tseng W-YIYI. Washout gradient in dynamic contrast-enhanced MRI is associated with tumor aggressiveness of prostate cancer. J Magn Reson Imaging 2012;36:912–9. doi:10.1002/jmri.23723.

[122]   Starobinets O, Simko JP, Kuchinsky K, Kornak J, Carroll PR, Greene KL, et al. Characterization and stratification of prostate lesions based on comprehensive multiparametric MRI using detailed whole-mount histopathology as a reference standard. NMR Biomed 2017;30:e3796. doi:10.1002/nbm.3796.

[123]   Przelaskowski PS, Życka-Malesa D, Mykhalevych I, Sklinda K, Artur. Przelaskowski. MRI imaging texture features in prostate lesions classification. EMBEC NBC 2017, 2017, p. 827–30. doi:10.1007/978-981-10-5122-7.

[124]   Sobecki P, Zycka-Malesa D˙, Mykhalevych I, Gora A, Sklinda K, Przelaskowski A. Feature extraction optimized for prostate lesion classification. Proc. 9th Int. Conf. Bioinforma. Biomed. Technol., 2017, p. 22–7. doi:10.1145/3093293.3093312.

[125]   Holtz JN, Silverman RK, Tay KJ, Browning JT, Huang J, Polascik TJ, et al. New prostate cancer prognostic grade group (PGG): Can multiparametric MRI (mpMRI) accurately separate patients with low-, intermediate-, and

high-grade cancer? Abdom Radiol 2017;43:702–12. doi:10.1007/s00261-017-1255-8.

[126]   Fehr D, Veeraraghavan H, Wibmer A, Gondo T, Matsumoto K, Vargas HA, et al. Automatic classification of prostate cancer Gleason scores from multiparametric magnetic resonance images. Proc Natl Acad Sci 2015;112:E6265–73. doi:10.1073/pnas.1505935112.

[127]   Le MH, Chen J, Wang L, Wang Z, Liu W, Cheng K-T (Tim), et al. Automated diagnosis of prostate cancer in multi-parametric MRI based on multimodal convolutional neural networks. Phys Med Biol 2017;62:6497–514. doi:10.1088/1361-6560/aa7731.

[128]   Wibmer A, Hricak H, Gondo T, Matsumoto K, Veeraraghavan H, Fehr D, et al. Haralick texture analysis of prostate MRI: utility for differentiating non-cancerous prostate from prostate cancer and differentiating prostate cancers with different Gleason scores. Eur Radiol 2015;25:2840–50. doi:10.1007/s00330-015-3701-8.

[129]   Li J, Weng Z, Xu H, Zhang Z, Miao H, Chen W, et al. Support Vector Machines (SVM) classification of prostate cancer Gleason score in central gland using multiparametric magnetic resonance images: A cross-validated study. Eur J Radiol 2018;98:61–7. doi:10.1016/j.ejrad.2017.11.001.

[130]   De Bruijne M. Machine learning approaches in medical image analysis: From detection to diagnosis. Med Image Anal 2016;33:94–7. doi:10.1016/j.media.2016.06.032.

[131]   Suzuki K. Overview of deep learning in medical imaging. Radiol Phys Technol 2017;10:257–73. doi:10.1007/s12194-017-0406-5.

[132]   Erickson BJ, Korfiatis P, Akkus Z, Kline TL. Machine Learning for Medical Imaging. Radiographics 2017;37:505–15. doi:10.1148/rg.2017160130.

[133]   Galloway MM. Texture analysis using gray level run lengths. Comput Graph Image Process 1975;4:172–9. doi:10.1016/S0146-664X(75)80008-6.

[134]   Haralick RM, Shanmugam K, Dinstein I. Textural features for image classification. IEEE Trans Syst Man Cybern 1973;3:610–21. doi:10.1109/TSMC.1973.4309314.

[135]   Saeys Y, Aki Inza I, Larrañ Aga P. A review of feature selection techniques in bioinformatics. Bioinforma Rev 2007;23:2507–17. doi:10.1093/bioinformatics/btm344.

[136]   Wang L, Wang Y, Chang Q. Feature selection methods for big data
        bioinformatics: A survey from the search perspective. Methods
        2016;111:21–31. doi:10.1016/j.ymeth.2016.08.014.

[137]   S. E. Viswanath. A Quantitative Data Representation Framework for
        Structural and Functional MR Imaging with Application to Prostate Cancer
        Detection. Rutgers University-Graduate School-New Brunswick, 2012.

[138]   Kotsiantis SB, Zaharakis I, Pintelas P. Supervised Machine Learning: A
        Review of Classification Techniques. Emerg Artif Intell Appl Comput Eng
        2007;160:3–24. doi:10.1115/1.1559160.

[139]   Erickson BJ, Korfiatis P, Kline TL, Akkus Z, Philbrick K, Weston AD.
        Deep Learning in Radiology: Does One Size Fit All? J Am Coll Radiol
        2018;15:521–6. doi:10.1016/j.jacr.2017.12.027.

[140]   Zbigniew Zdziarski. Why Deep Learning Has Not Superseded Traditional
        Computer Vision | Zbigatron 2018. https://zbigatron.com/has-deep-learning-
        superseded-traditional-computer-vision-techniques/ (accessed September 7,
        2018).

[141]   Mazurowski MA, Buda M, Saha A, Bashir MR. Deep learning in radiology:
        an overview of the concepts and a survey of the state of the art 2018;153:1–
        27.

[142]   Gupta V. Image Classification using Convolutional Neural Networks in
        Keras 2017. https://www.learnopencv.com/image-classification-using-
        convolutional-neural-networks-in-keras/ (accessed September 10, 2018).

[143]   Ronneberger O, Fischer P, Brox T. U-Net: Convolutional Networks for
        Biomedical Image Segmentation. Int Conf Med Image Comput Comput
        Interv 2015:234–41. doi:10.1007/978-3-319-24574-4_28.

[144]   James G, Witen D, Hastie T, Tibshirani R. An Introduction to Statistical
        Learning with Applications in R. vol. 64. Springer; 2014.
        doi:10.1016/j.peva.2007.06.006.

[145]   Grahn, Grahn, Hans; Geladi P, Geladi P. Techniques and Applications of
        Hyperspectral Image Analysis. John Wiley & Sons; 2007.
        doi:10.1002/9780470010884.

[146]   Arlot S, Celisse A. A survey of cross-validation procedures for model
        selection. Stat Surv 2010;4:40–79. doi:10.1214/09-SS054.

[147] Chicco D. Ten quick tips for machine learning in computational biology. BioData Min 2017;10:35. doi:10.1186/s13040-017-0155-3.

[148] Larose DT, Larose CD. Discovering Knowledge in Data: an Introduction to Data Mining. John Wiley & Sons; 2014. doi:10.1198/jasa.2005.s61.

[149] Jensen C, Korsager AS, Boesen L, Østergaard LR, Carl J. Computer Aided Detection of Prostate Cancer on Biparametric MRI Using a Quadratic Discriminant Model. Scand. Conf. Image Anal., vol. 10270, Springer, Cham; 2017, p. 161–71. doi:10.1007/978-3-319-59126-1_14.

[150] Afef L, Rania T, Hanen C, Lamia S, Ahmed BH. Comparison study for computer assisted detection and diagnosis "CAD" systems dedicated to prostate cancer detection using MRImp modalities. 2018 4th Int Conf Adv Technol Signal Image Process ATSIP 2018 2018:1–6. doi:10.1109/ATSIP.2018.8364468.

[151] Armato SG, Petrick NA, Drukker K. PROSTATEx: Prostate MR Classification Challenge (Conference Presentation). In: Armato SG, Petrick NA, editors. vol. 10134, International Society for Optics and Photonics; 2017, p. 101344G. doi:10.1117/12.2280374.

[152] Radtke JP, Boxler S, Kuru TH, Wolf MB, Alt CD, Popeneciu I V, et al. Improved detection of anterior fibromuscular stroma and transition zone prostate cancer using biparametric and multiparametric MRI with MRI-targeted biopsy and MRI-US fusion guidance. Prostate Cancer Prostatic Dis 2015;18:288–96. doi:10.1038/pcan.2015.29.

[153] Scialpi M, Falcone G, Scialpi P, D'Andrea A. Biparametric MRI: a further improvement to PIRADS 2.0? Diagn Interv Radiol 2016;22:297–8. doi:10.5152/dir.2016.15598.

[154] Weese J, Lorenz C. Four challenges in medical image analysis from an industrial perspective. Med Image Anal 2016;33:44–9. doi:10.1016/J.MEDIA.2016.06.023.

[155] Litjens G, Debats O, Barentsz J, Karssemeijer N, Huisman H. SPIE-AAPM PROSTATEx Challenge Data 2017. https://wiki.cancerimagingarchive.net/display/Public/SPIE-AAPM-NCI+PROSTATEx+Challenges (accessed October 13, 2017).

[156] Miotto R, Wang F, Wang S, Jiang X, Dudley JT. Deep learning for healthcare: review, opportunities and challenges. Brief Bioinform 2017. doi:10.1093/bib/bbx044.

[157]   Giganti F, Moore CM. A critical comparison of techniques for MRI-targeted biopsy of the prostate. Transl Androl Urol 2017;6:432–43. doi:10.21037/tau.2017.03.77.

[158]   Orczyk C, Hu YP, Gibson E, El-Shater Bosaily A, Kirkham A, Punwani S, et al. Should We Aim for the Centre of an Mri Prostate Lesion? Correlation Between Mpmri and 3-Dimensional 5Mm Transperineal Prostate Mapping Biopsies From the Promis Trial. J Urol 2017;197:e486. doi:10.1016/j.juro.2017.02.1160.

[159]   Singh R, Gosavi A, Agashe S, Sulhyan K. Interobserver reproducibility of Gleason grading of prostatic adenocarcinoma among general pathologists. Indian J Cancer 2011;48:488. doi:10.4103/0019-509X.92277.

[160]   Zhan Y, Feldman M, Tomaszeweski J. Registering Histological and MR Images of Prostate for Image-Based Cancer Detection. Int. Conf. Med. Image Comput. Comput. Interv., Springer, Berlin, Heidelberg; 2006, p. 620–8.

[161]   Wildeboer RR, Schalk SG, Demi L, Wijkstra H, Mischi M. Three-dimensional histopathological reconstruction as a reliable ground truth for prostate cancer studies. Biomed Phys Eng Express 2017;3:035014. doi:10.1088/2057-1976/aa7073.

[162]   Li L, Rusu M, Viswanath S, Penzias G, Pahwa S. Multi-modality registration via multi-scale textural and spectral embedding representations. Proc. SPIE 9784, Med. Imaging 2016 Image Process., vol. 9784, 2016, p. 1–12. doi:10.1117/12.2217639.

[163]   Kalavagunta C, Zhou X, Schmechel SC, Metzger GJ. Registration of In Vivo Prostate MRI and Pseudo-Whole Mount Histology Using Local Affine Transformations Guided by Internal Structures (LATIS). J Magn Reson Imaging 2015;41:1104–14. doi:10.1002/jmri.24629.

[164]   Cornford P, Bellmunt J, Bolla M, Briers E, De Santis M, Gross T, et al. EAU-ESTRO-SIOG Guidelines on Prostate Cancer. Part II: Treatment of Relapsing, Metastatic, and Castration-Resistant Prostate Cancer. Eur Urol 2017;71:630–42. doi:10.1016/j.eururo.2016.08.002.

[165]   Alfano R, Soetemans D, Bauman G, Gibson E, Gaed M, Moussa M, et al. Development of a computer aided diagnosis model for prostate cancer classification on multi-parametric MRI. In: Mori K, Petrick N, editors. Med. Imaging 2018 Comput. Diagnosis, vol. 10575, SPIE; 2018, p. 40. doi:10.1117/12.2293341.

[166] Roethke MC, Kuru TH, Mueller-Wolf MB, Agterhuis E, Edler C, Hohenfellner M, et al. Evaluation of an automated analysis tool for prostate cancer prediction using multiparametric magnetic resonance imaging. PLoS One 2016;11:1–16. doi:10.1371/journal.pone.0159803.

[167] Edmund JM, Nyholm T. A review of substitute CT generation for MRI-only radiation therapy. Radiat Oncol 2017;12:28. doi:10.1186/s13014-016-0747-y.

[168] Valle LF, Greer MD, Shih JH, Barrett T, Law YM, Rosenkrantz AB, et al. Multiparametric MRI for the detection of local recurrence of prostate cancer in the setting of biochemical recurrence after low dose rate brachytherapy. Diagnostic Interv Radiol 2018;24:46–53. doi:10.5152/dir.2018.17285.

APPENDICES

Appendix A. Paper A

Computer Aided Detection of Prostate Cancer on Biparametric MRI Using a Quadratic Discriminant Model

Carina Jensen, Anne Sofie Korsager, Lars Boesen, Lasse Riis Østergaard and Jesper Carl

The layout has been revised.

Appendix B. Paper B

Assessment of Prostate Cancer Prognostic Gleason Grade Group using Zonal Specific Features Extracted from Biparametric MRI – a Machine Learning Approach

Carina Jensen, Jesper Carl, Lars Boesen, Niels Christian Langkilde and Lasse Riis Østergaard

The layout has been revised.

Appendix C. Paper C

Zonal Segmentation of the Prostate in 1.5T and 3T MRI using a Convolutional Neural Network

Carina Jensen, Kristine Storm Sørensen, Cecilia Klitgaard Jørgensen, Camilla Winther Nielsen, Pia Christine Høy, Niels Christian Langkilde and Lasse Riis Østergaard

The layout has been revised